LAND AND WATER
www.csiro.au

Using Numerical Groundwater Modelling to Constrain Flow Rates and Flow Paths in the Surat Basin through Environmental Tracer Data

Adam Siade, Henning Prommer, Axel Suckow, Matthias Raiber
July 2018

ISBN (print): 978-1-4863-1014-2

ISBN (online): 978-1-4863-1015-9

Citation

Siade, Adam, Prommer, Henning, Suckow, Axel, Raiber, Matthias (2018): Using Numerical Groundwater Modelling to Constrain Flow Rates and Flow Paths in the Surat Basin through Environmental Tracer Data. Final Report. CSIRO, Australia.

Copyright and disclaimer

Important disclaimer

Content

Figures

Tables

Acknowledgments

This report was supported by the Gas Industry Social and Environmental Research Alliance (GISERA). GISERA is a collaboration between CSIRO, Commonwealth and state governments and industry established to undertake publicly-reported independent research. The purpose of GISERA is to provide quality assured scientific research and information to communities living in gas development regions focusing on social and environmental topics including: groundwater and surface water, biodiversity, land management, the marine environment, and socio-economic impacts. The governance structure for GISERA is designed to provide for and protect research independence and transparency of research. Visit gisera.csiro.au for more information about GISERA's governance structure, projects and research findings.

The authors thank Origin Energy for their knowledge and understanding of the investigated aquifers and the Office of Groundwater Impact Assessment for their support with their Surat Cumulative Management Area (CMA) model.

This report was subject to CSIRO-internal review. We thank our internal reviewers Dirk Mallants and Jim McCallum for their rapid and constructive feedback.

Executive summary

Background

Groundwater flow models are routinely used to gain a better quantitative understanding of groundwater systems and provide the basis for important water resources management decisions. Due to the growing coal seam gas (CSG) industry in the Surat and Bowen sedimentary basins, the Surat cumulative management area (CMA) was established to assess and manage the associated water level impacts. Over the past years, the Office of Groundwater Impact Assessment of Queensland (OGIA) has established a comprehensive conceptual and numerical groundwater flow modelling framework to underpin the assessment and management of the Surat CMA (*OGIA*, 2016a; b; c). Although a significant amount of data and expert knowledge has been employed in the development of this sophisticated modelling framework, some parameter and conceptual uncertainties still persist, especially for the deeper Hutton Sandstone and Precipice Sandstone aquifer systems and with respect to defining natural, pre-development groundwater flow conditions prior to any anthropogenic disturbances. This is due to (i) the limited availability of hydraulic head data for these aquifers, especially for pre-development conditions, and (ii) due to the correlations induced by using hydraulic head data as the primary constraint for calibrating a model. Characterising these deeper aquifers and developing a robust quantitative understanding of them is becoming increasingly important when assessing the potential impacts of CSG operations on the Hutton Sandstone, as well as separating these impacts from those associated with both farming-related extraction and re-injection of CSG co-produced waters on the Precipice Sandstone aquifers. A major conceptual and/or parametric uncertainty in these deeper aquifers is associated with the apparent contradiction between, (1) the conceptual understanding that recharge enters the Surat Basin through outcrop areas, eventually contributing recharge to the Great Artesian Basin, and (2) the fact that the observed potentiometric surface indicates that groundwater is flowing toward, and discharging from, the outcrop areas themselves. This major discrepancy has motivated the collection of new environmental tracer concentration data (^{36}Cl, ^{14}C, helium, etc.) in these aquifers (*Suckow et al*, 2018) for the present GISERA project to complement earlier collected data (*Suckow et al*, 2016) and to underpin a more robust data interpretation. Environmental tracers can provide important information about groundwater “age”, or residence times, that can be used to deduce flow velocities and hence, hydraulic properties of the aquifers. In this study, a three-dimensional numerical modelling approach was employed to jointly simulate groundwater flow and the transport of multiple environmental tracers. The Surat CMA model developed by *OGIA* (2016c) was used as the basis for developing flow fields in the Hutton Sandstone and Precipice Sandstone including the Evergreen Formation which separates them. The subsequent joint inversion of hydraulic head and environmental tracer data was then used to derive an improved, more robust parameterisation of the aquifer properties and to reduce model uncertainty.

- A numerical modelling approach was developed to simulate the physico-chemcial behaviour of the environmental tracers ^{36}Cl and ^{14}C in the deeper aquifer sections of the Surat Basin.
- Newly and previously collected ^{36}Cl and ^{14}C data, as well as hydraulic head data, were used as joint model calibration targets to constrain the conceptualisation and parameterisation of a numerical model representing pre-development groundwater flow behaviour.
- The regional groundwater flow of the Surat CMA, as developed by OGIA (2016c), was used as a starting point for model construction and for generating flow fields.
- The calibrated model re-produces ^{36}Cl very well in the Hutton Sandstone aquifer. The parameter estimation results will inform future versions of the OGIA model.
- Due to the relatively old age of the groundwater, ^{14}C data was insensitive to many of the hydraulic parameters but may be more useful for local-scale models at the outcrops.
- Mean age simulations quantify the effects of both mixing and subsurface production on interpreting groundwater ages from ^{36}Cl data.
- Groundwater flow directions are complex but it is very likely that groundwater, which has recharged at the aquifer outcrops, discharges primarily through the eastern outcrops near the Dawson River.

Key results

The analysis conducted in this study demonstrates that the information content associated with environmental tracer observations can be significant. A sophisticated workflow was developed and tested for the extraction and implementation of flow fields from the Surat CMA model (*OGIA*, 2016c). This procedure allowed for the employment of the widely used solute transport code MT3DMS for the simulation of the reactive transport of ^{36}Cl and ^{14}C.

The calibrated model reproduced the ^{36}Cl data well and provided a range of new insights into aquifer properties. The results indicate, for example, that the hydraulic conductivity in the Lower Hutton Sandstone may be greater than current estimates. However, the hydraulic properties of the Precipice Sandstone still remain uncertain due to the insensitivity of the ^{14}C data and perhaps due to conceptual model assumptions about coverage of outcrop areas. This is likely due to the relatively old age of much of the groundwater in both aquifers of interest, which may be beyond the age limit of ^{14}C in the interior of the basin.

Using the calibrated reactive transport model, mean age simulations demonstrate the significant impact of mixing and ^{36}Cl production on the interpretation of groundwater age using simplified models. For example, the simulated mean age in the Lower Hutton Sandstone near the Dawson River is about ten times larger than the groundwater age interpreted from the simplest of assumptions.

Conclusion and recommendations

Overall, the results show that both the potentiometric surface and the observed environmental tracer data can be simultaneously reproduced by the three-dimensional numerical model. The insights gained form this numerical modelling study also highlights that the flow system is far too complex to be interpreted by simplistic one-dimensional approaches. Recharge in the Surat Basin is likely being discharged to the eastern outcrop areas near the Dawson River, but future research is required to better quantify localised net recharge rates and the possibility that recharge in the Surat Basin also contributes recharge to the Great Artesian Basin.

Due to the significant amount of information contained in environmental tracers, the joint data collection and numerical modelling approach illustrated by this study could improve the conceptualisation and parameterisation of many other groundwater systems. Measuring environmental tracers in the field is expensive and often requires significant expertise to be sampled properly. As a result, the location and type of future measurements should always be selected very carefully, which may not be straightforward. However, with emerging data worth and experimental design techniques, numerical models can increasingly be used to determine where and what data type should be collected to maximise the information acquired.

While beyond the scope of the present study, the direct simulation of helium as an additional environmental tracer has significant potential for acquiring information for both younger waters and the very old groundwater in deeper aquifer systems beyond the temporal reach of ^{36}Cl and ^{14}C data. This is because changes in the accumulation and transport of helium is likely to be sensitive to the entire flow field regardless of age, i.e., the distribution of helium in very old groundwater (more than one million years) may be highly variable, where for example, ^{36}Cl would be relatively uniform (at its average secular equilibrium) and ^{14}C would be negligible (at about 0 pmc). Although ^{36}Cl has a long enough half-life to provide some information on old groundwater (up to a million years), due to the relatively short half-life of ^{14}C, it may not be informative on a regional scale where the bulk of the groundwater in the Surat Basin is well over 50,000 years old. However, the development of one or more two-dimensional, cross-sectional reactive transport models extending from the Hutton and Precipice Sandstone outcrops into the interior of the basin, along selected flow paths, could be constructed to make effective use of the ^{14}C data near outcrops and better estimate local-scale net recharge rates.

1 Introduction

Groundwater flow models are routinely used to gain a better quantitative understanding of groundwater systems and provide the basis for important water resources management decisions. Due to the growing coal seam gas (CSG) industry in the Surat and Bowen sedimentary basins, the Surat cumulative management area (CMA) was established to assess and manage the associated water level impacts. Over the past years OGIA has established a comprehensive conceptual and numerical groundwater flow modelling framework to underpin the assessment and management of the CMA (*OGIA*, 2016a). The established numerical modelling framework integrates a vast array of hydrological, geological and hydrogeological data to allow for the quantification of historic and future groundwater flow rates and water levels. During the construction of such a groundwater flow model the magnitude and the spatial distribution of hydrogeological parameters are initially only conceptualised and are considered to be uncertain. Typically, the model construction is therefore followed by a model calibration procedure during which model parameters are systematically adjusted until the model predictions fit historical measurements.

Currently, conventional groundwater model calibration procedures rely largely on the use of observed hydraulic heads as model calibration constraints. Although some flux conditions are used as calibration constraints, the OGIA's CMA model primarily relies largely on a number of historic groundwater level data which were used to constrain the conceptualisation and parameterisation of the numerical model (*OGIA*, 2016c). However, model calibration based on hydraulic head measurements alone can suffer from non-uniqueness resulting in potentially significant predictive uncertainty (*Konikow and Bredehoeft*, 1992; *Zimmerman et al..*, 1998). This can in particular be a problem when model predictions are highly sensitive to processes and parameters that play a less prominent role in providing a good agreement between simulation results and historical data. For example, models developed for the resources industries to simulate dewatering impacts are relatively sensitive only to model parameters that describe the storage behaviour of the aquifer system in response to dewatering or depressurisation. On the other hand, predictions that simulate the long-term recovery after dewatering/depressurisation activities have been terminated are relatively more sensitive to estimated groundwater recharge rates, which often remain uncertain as the transient changes induced by dewatering and depressurisation are not highly sensitive to the estimated recharge rates. To reduce this uncertainty, understanding and quantifying the distribution of groundwater ages within an aquifer system provides a significant potential to better constrain estimates of groundwater recharge and flow rates (*Cook and Robinson*, 2002; *Solomon et al..*, 1993; *Vogel et al..*, 1974) and therefore improve the reliability of groundwater flow models (*Michael and Voss*, 2009; *Reilly et al..*, 1994; *Sanford*, 2011; *Sanford et al..*, 2004; *Turnadge and Smerdon*, 2014; *Yager et al..*, 2013).

Groundwater age distributions, or residence times and flow paths, can be inferred from measured groundwater tracers such as ^{36}Cl, ^{14}C, ^{4}He, ^{81}Kr, etc. Many studies have used groundwater tracers to infer ages throughout the Great Artesian Basin (*Bentley et al.*, 1986; *Torgersen et al.*, 1991; *Love et al.*, 2000; *Lehman et al.*, 2003; *Mahara et al.*, 2009) and have discussed the numerous limitations associated with inferring groundwater ages, sometimes suggesting the use of other metrics instead, e.g., flow velocity. However, by incorporating raw groundwater tracer data directly into a regional-scale numerical modelling framework, many of these limitations can be alleviated (*Suckow*, 2014). This is a novel approach that has received little attention, with the few existing studies in the literature using relatively simplified models with at most two-dimensions (*Castro and Goblet*, 2003; *Patterson et al.*, 2005).

The present GISERA study was specifically designed to explore the benefits of using environmental tracer data as model calibration constraints within a subdomain of OGIA's groundwater flow model. Relying on a unique dataset of existing and newly collected environmental tracer data (*Ransley and Smerdon*, 2012; *Feitz et al.*, 2014; *Suckow et al..*, 2016; 2018), this study developed the necessary tools to integrate the simulation of selected environmental tracers into a comprehensive modelling framework that jointly uses observed hydraulic heads and observed environmental tracer concentrations. While apparent groundwater ages as inferred from environmental tracer data have occasionally been used as additional independent observations to further constrain and calibrate numerical groundwater models (*Leray et al..*, 2012; *Weiss and Smith*, 1998), the present modelling study is unique in that it uses, for the first time, a combination of environmental tracers that directly characterise old and very old waters (up to millions of years), at the sedimentary basin scale, without the need for interpreting an apparent groundwater age. The study is focussed specifically on groundwater flows within the Hutton and Precipice Sandstone aquifer systems within the CMA, for which effective groundwater recharge rates are still relatively uncertain with estimates ranging by over an order of magnitude based on interpretation of tracer data (*Suckow et al.*, 2016; 2018) and chloride mass balance (*OGIA*, 2016a). However, while beyond the scope of the present work, the methods and modelling approaches developed in this study will be transferrable to other subdomains of the Surat Basin and elsewhere.

2 Methods

2.1 Study area

Covering an area of 440,000 km^2, the Surat and Bowen basins are located in south-central Queensland, Australia, and are the primary target for CSG extractions within the Surat CMA. OGIA conducted an extensive geologic investigation to develop a three-dimensional spatial representation of the system's regional stratigraphy (*OGIA*, 2016a; b). This stratigraphy included the Condamine River alluvium, Main Range Volcanics, Surat and Bowen basins (Figure 2.1). A lithostratigraphic approach was used to develop layers in the Surat and Bowen basins by defining boundaries between geologic formations based on major changes in the depositional environment.

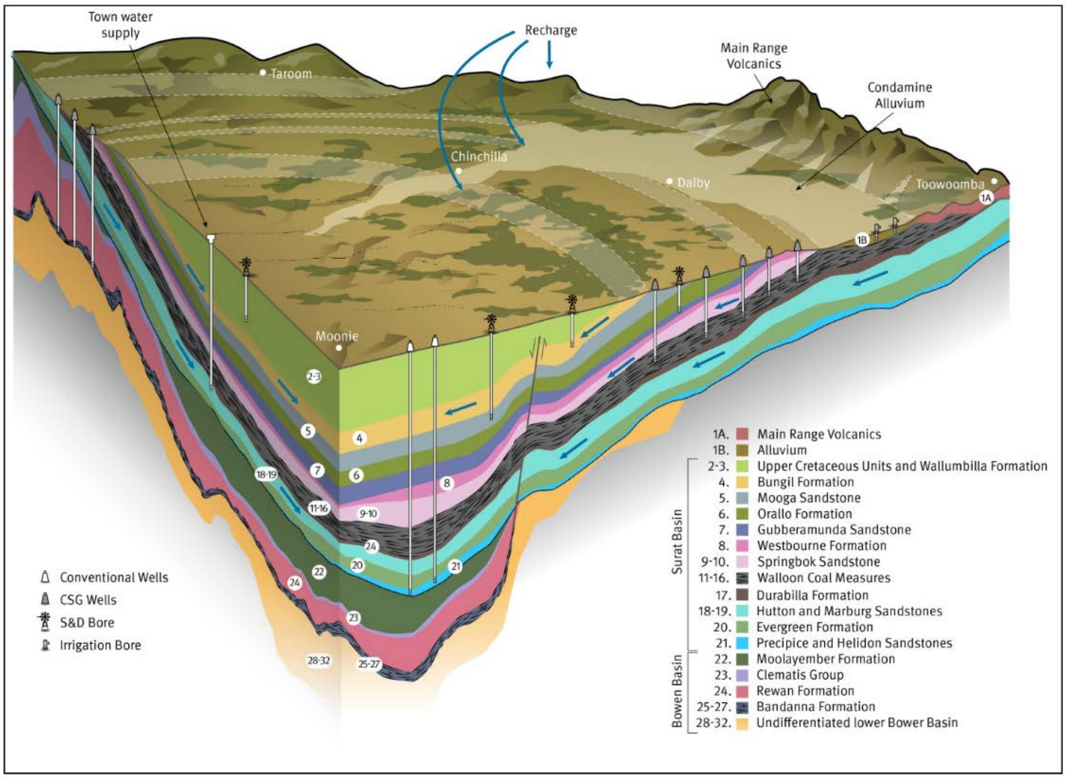

Figure 2.1: Conceptual model of the groundwater systems in the Surat Cumulative Management Area (*OGIA* 2016a; b; c)

The Surat Basin is considered part of the Great Artesian Basin (GAB), with the western margins of the Surat and Bowen basins being hydraulically connected to the Eromanga Basin of the GAB (*Habermehl*, 1980; *Radke et al.*., 2000). Along a portion of the southern boundary, the Surat Basin connects far into New South Wales, including the Coonamble Embayment and the Oxley Basin, which overly the Gunnedah Basin (*Habermehl*, 1980). The deepest formation in the Surat Basin is the Precipice Sandstone, which unconformably overlies the Bowen Basin (Figure 2.1). The Precipice Sandstone is hydraulically disconnected from the overlying Hutton Sandstone by both a shale-rich layer and by the Evergreen Formation aquitard (*Hodgkinson et al.*, 2010).

There are two known and noteworthy structural faults at the margins of the Mimosa Syncline. Both faults trend north-south and result in only minor deformations and displacements in the system. The faults are named the Hutton-Wallumbilla fault in the west, the Moonie-Goondiwindi and Burunga-Leichhardt fault system in the east (referred together as the Burunga-Leichhardt fault) (*OGIA*, 2016a; b).

2.1.1 HYDROGEOLOGICAL CHARACTERISTICS OF THE HUTTON AND PRECIPICE AQUIFERS

The quality of groundwater among the two investigated aquifers, i.e., the Hutton and Precipice sandstone aquifers, is better in the Precipice Sandstone, as the Hutton Sandstone has generally higher salinity (*Ransley et al.*., 2015; *Raiber and Suckow*, 2017; *Suckow et al.*., 2016; 2018). The Hutton Sandstone also has a lower yield, as suggested by extensive sediment core testing that resulted in a relatively wide range of hydraulic conductivity estimates from 10-5 to 1 m/d in both horizontal and vertical directions (*APLNG*, 2014). The hydraulic conductivity estimates for the Precipice Sandstone ranged from 0.001 to 10 m/d (*APLNG*, 2014).

Recharge for the Hutton and Precipice Sandstone aquifers is generally assumed (*Kellett et al.*., 2003) to occur in the regions where the aquifers outcrop, i.e., are expressed at land surface. Due to the sedimentation history, these outcrop areas take an upside-down "U" shape around Taroom and Injune (Figure 2.2).

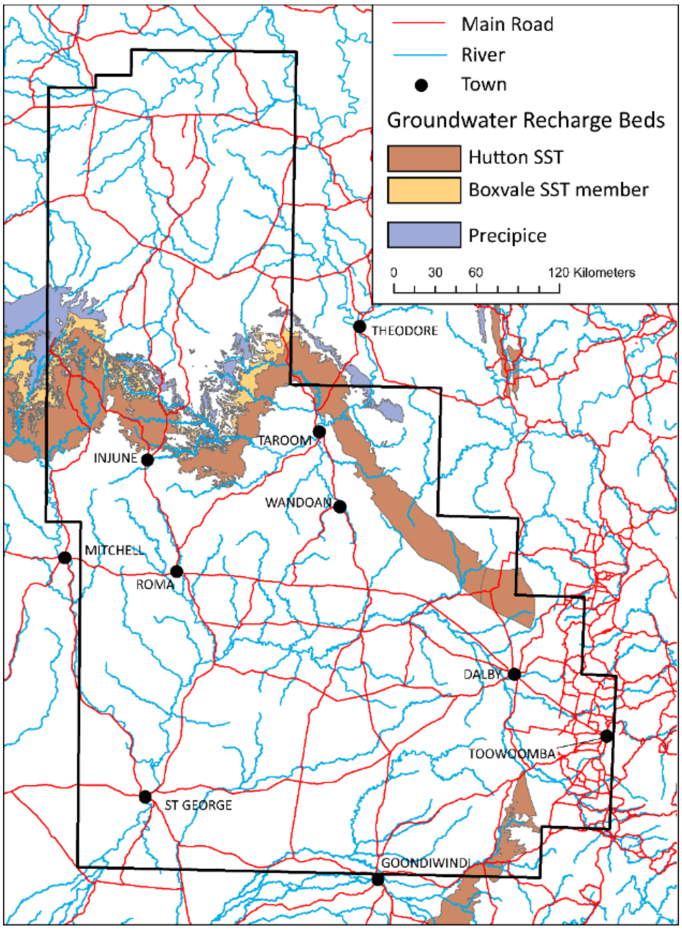

Figure 2.2: Surat CMA and planar extent of recharge areas (i.e., outcrop areas).

A potentiometric surface was recently developed by *Hodgkinson et al.* (2010), which indicates that the major recharge areas are within the northern and eastern outcrop areas (Figure 2.3). Inferred groundwater flow lines indicate that groundwater flow fans out in several directions from these areas, exiting the basins as either interflow to the south, or as discharge to the Dawson River in the outcrop areas of the north-east. The latter, which is counterintuitive, is supported by an observed groundwater depression in the Hutton Sandstone near Taroom, with similar results for the Evergreen Formation and Precipice Sandstone (*Hodgkinson et al.*, 2010). Although the GAB is hydraulically connected in the west, groundwater flow across this boundary is generally assumed to be negligible, especially prior to the more recent anthropogenic extractions (*OGIA*, 2016a; b; c).

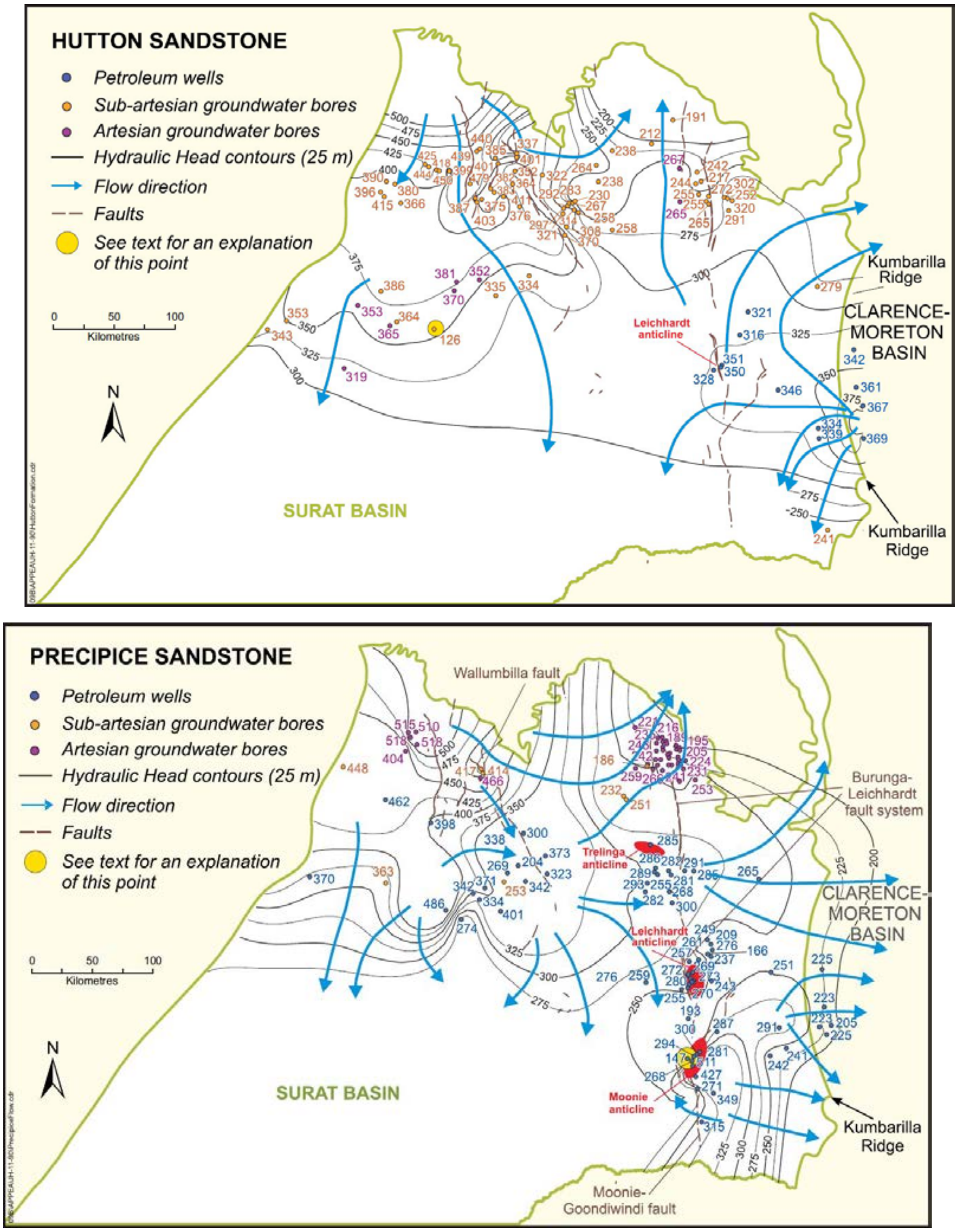

Figure 2.3: Inferred potentiometric surface of the Hutton and Precipice Sandstone aquifers (*Hodgkinson et al.*, 2010)

2.2 Environmental Tracer Sampling Campaign

The discrepancy between the map of hydraulic heads developed by *Hodgkinson et al.* (2010) and the general understanding that the Hutton and Precipice Sandstone aquifers are recharge areas, with a groundwater flow towards the Great Artesian Basin, motivated several different environmental tracer studies. The key question that motivated this first study was whether the historical groundwater flow in the Hutton Sandstone was in fact occurring in southerly direction and thus contributing recharge to the GAB. This resulted in a sampling campaign, undertaken in 2013 and published in 2016 (*Suckow et al.*, 2016), focused on the Hutton Sandstone. The initial idea was to sample two north-south transects for as many environmental tracers as feasible and to determine the historical flow direction, i.e., the flow direction prior to any significant anthropogenic influence. Concentrations of environmental tracers such as tritium, ^{14}C, and ^{36}Cl are often considered to represent the “age” of a groundwater sample, which can be used to conceptually determine flow direction. Given that environmental tracer data for “old tracers” represent the long-term groundwater flow behaviour rather than the current flow behaviour, a southerly flow direction should have shown a north-to-south trend of increasing groundwater ages. However, it should be noted that the interpretation of a groundwater "age" can be misleading, as in reality any water sample typically represents a mixture of waters with differing residence times, i.e., different ages (*IAEA*, 2013; *Suckow*, 2014).

The analysis of the sampled environmental tracer data did not show the anticipated clear north-to-south trend in interpreted groundwater age. This indicated that a single, simplistic one-dimensional flow direction was an inadequate conceptualisation of the system and that further analysis was required. *Suckow et al.*, (2016) hypothesised a general trend of increasing groundwater ages with increasing distance between the sampled well and the nearest Hutton Sandstone outcrop point. This trend was in fact evident for each individual tracer; however, the flow velocities inferred from each tracer (^{14}C and ^{36}Cl) differed by one order of magnitude. *Suckow et al.* (2016) found that this discrepancy can, however, be reconciled under the assumption that the Hutton Sandstone is a double porosity system in which groundwater flow occurs only in a small fraction ("mobile fraction") of the whole formation. The data suggested that at most 20% of the thickness acts as the mobile fraction. This was in agreement with the sedimentological description of the genesis of this formation (*Guiton et al.*, 2015). However, the actual groundwater velocity could not be uniquely determined by fitting the tracer data alone; only the product of (1) the effective thickness in which the aquifer groundwater flow takes place, (2) porosity, and (3) groundwater velocity could be determined. In other words, halving the effective thickness and doubling the groundwater velocity would give the same fit. Despite this limitation, this analysis provided a first quantitative estimate of the effective deep recharge that entered the Hutton Sandstone under pre-development conditions. The estimated rates were 30 times lower than earlier estimates that were based on a chloride mass balance. The description of the Hutton Sandstone as a double porosity system also agreed with findings of a numerical study, where the environmental tracer results could not be reproduced with a simple particle tracking approach, which only accounts for purely advective transport (*Sreekanth and Moore*, 2015).

This first study (*Suckow et al.*, 2016) also revealed several open questions. Very little is known about the deeper Precipice Sandstone and its flow dynamics and recharge mechanism which may provide insight into the question of flow directions in the Surat CMA. This is also becoming increasingly important because the Precipice Sandstone is now the target of large-scale re-injection of CSG process water. Furthermore, the Precipice Sandstone aquifer also has significance for the local farming industry given that farmers have started to pool their resources and drill deep and expensive wells into the Precipice Sandstone. The motivation for this is two-fold. First, the often-targeted Hutton Sandstone generally has a higher salinity and, secondly, its water levels have been observed to steadily decline. Since very few environmental tracer data exist for the deeper Precipice Sandstone, little can be deduced about its dynamics and hence more data is required.

To fill these data gaps, a second study was conducted within the current GISERA project. As part of this study, hydrochemical and environmental tracer data were collected in 2017 with a focus on the Precipice Sandstone (*Raiber and Suckow*, 2017; *Suckow et al.*, 2018). This sampling campaign suggested rather high flow velocities to occur in the Precipice Sandstone and groundwater ages of less than 40,000 years. This campaign also closed some data gaps in the Hutton Sandstone, especially with respect to tracer data for locations in the vicinity of the recharge areas. Both studies together have also given insight into helium accumulation rates within the two aquifers. The interpreted helium concentrations were consistent with the findings from the other tracers. The helium data also suggested areas in the western part of the Mimosa Syncline, close to the Hutton-Wallumbilla fault system, where deeper and older groundwater appears to ascend (*Suckow et al.*, 2018). Complementing the field data collection and interpretation, a trial study used quartz grains as proxies for the helium concentration in pore waters and to provide formation scale transmissivity values to assess connectivity between the Hutton Sandstone, the Precipice Sandstone, and the Walloon Coal Measures (*Smith*, 2015).

Altogether, these studies delivered some of the first estimates of deep recharge and suggested the subsequent use of the environmental tracers ^{14}C, ^{36}Cl and helium as calibration targets for a more detailed numerical study. This approach would alleviate the limitations of assuming a single one-dimensional flow direction, or individual flow directions for each sample, by including the full geometry and flow path distributions of the entire three-dimensional system.

2.3 Development of Model Framework

The simultaneous simulation of the transport and fate of multiple environmental tracers for old and very old groundwaters on the scale of the Surat CMA has not been previously conducted in the literature and remains a topic of advanced research. The main hypothesis of the present study is that such reactive transport simulations may have significant impacts on the reduction of predictive uncertainty of the underlying groundwater flow models. In order to conduct such an analysis, an accurate simulator of the groundwater flow field is required along with a set of suitable simplifying assumptions associated with the simulation of the reactive transport of the considered tracers. Within the scope of the present study the developed model framework included the simulation of the environmental tracers ^{14}C and ^{36}Cl. In principle, the numerical simulations of the reactive transport of these environmental tracers relied on OGIA's conceptual and numerical flow model framework. However, as discussed below, a range of utilities had to be developed and code modifications undertaken in order to allow for the efficient and practical construction and (re-)parametrisation of groundwater flow fields. This resulted in the development of numerically efficient surrogate models for groundwater flow and reactive environmental tracer transport in the Surat CMA. The model modifications and development had to be made in order to (1) extract the flow fields of interest from OGIA's Surat CMA model (from the Hutton Sandstone to the Precipice Sandstone), and (2) develop and test suitable, tracer-specific reactive transport modelling approaches.

2.3.1 OGIA'S REGIONAL GROUNDWATER FLOW MODEL FOR THE SURAT CMA

OGIA has conducted an extensive suite of analyses to understand the Surat Basin flow system and subsequently, to develop a numerical groundwater flow model (*OGIA*, 2016c). This model is designed to simulate the historical hydraulic conditions, within a reasonable degree of accuracy, as well as to make future predictions of the hydraulic system behaviour in response to anthropogenic influences, including CSG operations. In this section, a brief review of the current construction of OGIA's groundwater flow model is provided, with a focus on the Hutton and Precipice Sandstone aquifers as well as the Evergreen Formation; see OGIA (2016c) for further details.

Model Software, Spatial Extent and Discretisation

The groundwater flow model developed by OGIA is constructed using the unstructured-grid version of the U.S. Geological Survey (USGS) public domain software MODFLOW-USG (*Panday et al.*, 2017). A primary feature of this software is the ability to develop complex model grids that are not necessarily rectilinear; for example, Voronoi polygons can be used for variable grid resolution around specific hydrologic features such as rivers. This feature is, however, not employed in the Surat Basin groundwater flow model, which uses a rectilinear grid with square model cells, but may be explored in future versions of the model (*OGIA*, 2016c). MODFLOW-USG can also allow for vertical flow through layers that do not exist or are "pinched-out". For example, if a particular aquitard is modelled as layer 2, but does not exist in certain portions of the model domain, MODFLOW-USG can connect layers 1 and 3 directly without the need for layer 2 to be active. This is an important feature for the Surat Basin under the Condamine River Alluvium and Main Range Volcanics (among other areas) (*OGIA*, 2016c). However, this feature is largely not present from the Hutton Sandstone down to the Precipice Sandstone.

In addition to pinched-out layers, MODFLOW-USG also provides significant flexibility in model cell connections which is highly valuable along fault structures. Flow can be facilitated vertically by faults across many aquifers in the Surat Basin, and MODFLOW-USG is used to simulate this by connecting fault model cells with multiple model layers that are juxtaposed by fault displacement (*OGIA*, 2016c). This was applied to the Hutton-Wallumbilla and Burunga-Leichhardt faults discussed in the previous section. MODFLOW-USG is also used in the Surat Basin groundwater flow model to account for additional affects such as dual phase flow, dual porosity, etc. Finally, OGIA has worked with the developers of MODFLOW-USG to produce additional, site-specific modifications such as derating pumping wells, descending drains (for multi-node wells), etc., for the purposes of simulating CSG operations.

The hydrostratigraphy of the model domain is based on the three-dimensional geological model and consists of 32 layers. The numerical model layers and the aquifers which they represent are depicted in Figure 2.1. The Hutton Sandstone was subdivided into two layers, entitled the Upper (layer 18) and Lower (layer 19) Hutton, due to the vertical heterogeneity observed in their hydraulic properties; two distinct differences were observed based on geophysical log interpretations (*OGIA*, 2016c). Therefore, the primary model layers of interest for this study are layers 18-21, where the Evergreen Formation and Precipice Sandstone comprise layers 20 and 21, respectively.

The lateral extent of the model domain largely coincides with the Surat CMA. The model extends outside the Surat CMA in the west and south to account for the hydraulic connections in these directions. From the plan view, the width and height of the model is about 460 and 650 km, respectively. The model grid is discretised into square 1.5 km × 1.5 km model cells, resulting in 433 rows and 306 columns and about 1.2 million active model cells. The planar extent of the Upper/Lower Hutton Sandstone, Evergreen Formation, and Precipice Sandstone is about 140, 139, 135, and 101 × 103 km2; Figure 2.4 depicts the areal extent of these model layers compared to the overall extent of the entire model.

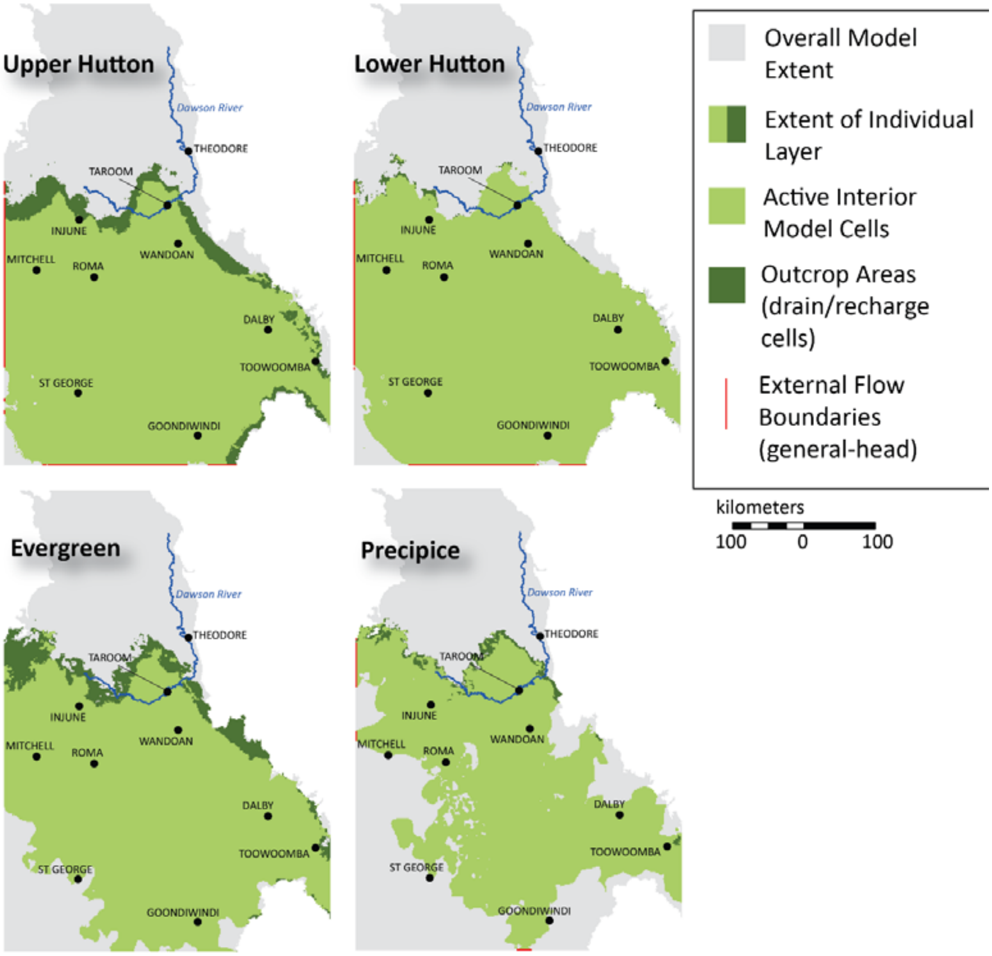

Figure 2.4: Spatial extent and boundary conditions of the Hutton Sandstone, Evergreen Formation, and Precipice Sandstone model layers for the numerical model developed by OGIA (*OGIA*, 2016c).

Temporal Discretisation

The simulation used for calibration of the Surat CMA model consists of three stages (*OGIA*, 2016c). The first simulation is a steady-state simulation that represents the hydrogeological conditions in 1947 when no significant anthropogenic groundwater extractions occurred, i.e., pre-development conditions. The second simulation is also a steady-state simulation which represents conditions in 1995. This simulation includes some anthropogenic extractions while CSG extractions had not yet started. The third simulation is a transient simulation that extends from the 1995 simulated conditions to 2014. This third simulation includes the spatially and temporally variable extraction from CSG operations. For the purposes of this study, only the pre-development simulation was used to simulate environmental tracer transport. Neglecting the transient groundwater flow conditions that occurred over the last few decades assumes that the concentrations of the investigated old and very old environmental tracers have not significantly changed during this period. In other words, today's observed spatial pattern of environmental tracer concentrations in the Hutton and Precipice is very similar to the pattern that would have been observed in 1947. Given the spatial scale of the model and the focus on old tracers, this assumption is most likely warranted as all the considered environmental tracers would not have moved over any significant distance during this period, despite the changes in hydraulic heads and flow rates that were induced by the various groundwater extractions.

Model Boundary Conditions

The discussion on boundary conditions here pertains only to the 1947 steady-state simulation, as the other two simulation periods are not considered in this study. The lateral boundaries of the overall model domain in the northwest and southeast are assumed to be no-flow boundaries (Figure 2.4). Each layer may be subject to four boundary types, (1) no-flow, (2) drainage, (3) general-head, and (4) recharge. A no-flow boundary exists along the faces of model cells that reside on the edge of a model layer, and do not contain recharge, drain or general-head boundary conditions.

The general-head boundaries (GHB's) simulate lateral groundwater flow into, or out of, a model layer associated with the GAB in the west, or the connections to groundwater basins in the south (Figure 2.4). The reference head assigned to the western GHB's was set to the simulated values obtained from an earlier version of the model, which assumed a no-flow condition further west of the current boundary (*GHD*, 2012). The corresponding conductance was calculated based on the estimated hydraulic properties, and distance between the previous model and current model's boundary locations. The reference head assigned to the southern GHB's was set to the land surface elevation and the associated conductance was calibrated during the development of the current Surat CMA model (*OGIA*, 2016c).

Recharge is applied on the outcrop areas of the Hutton Sandstone down to the Precipice Sandstone (Figure 2.4). The recharge rates were initially estimated via chloride mass balance at specific point locations followed by a subsequent interpolation over the outcrop areas (Figure 2.5) (*OGIA*, 2016a). Recharge is applied as a constant specified flux for the 1947 steady-state simulation. It is noteworthy that a substantial portion of this recharge is rejected to the surrounding shallow systems, which are represented as drains. That is, the model grid cells representing outcrop areas not only receive recharge, but they are also defined as drains, i.e., the spatial extent of the applied recharge is equivalent to the spatial extent of the simulated drains (Figure 2.5). The drain elevations are based on land surface conditions, and the conductance values are set to a spatially constant value of 5,000 m^2/d, which provides little impedance on the outflow of groundwater (*OGIA*, 2016c).

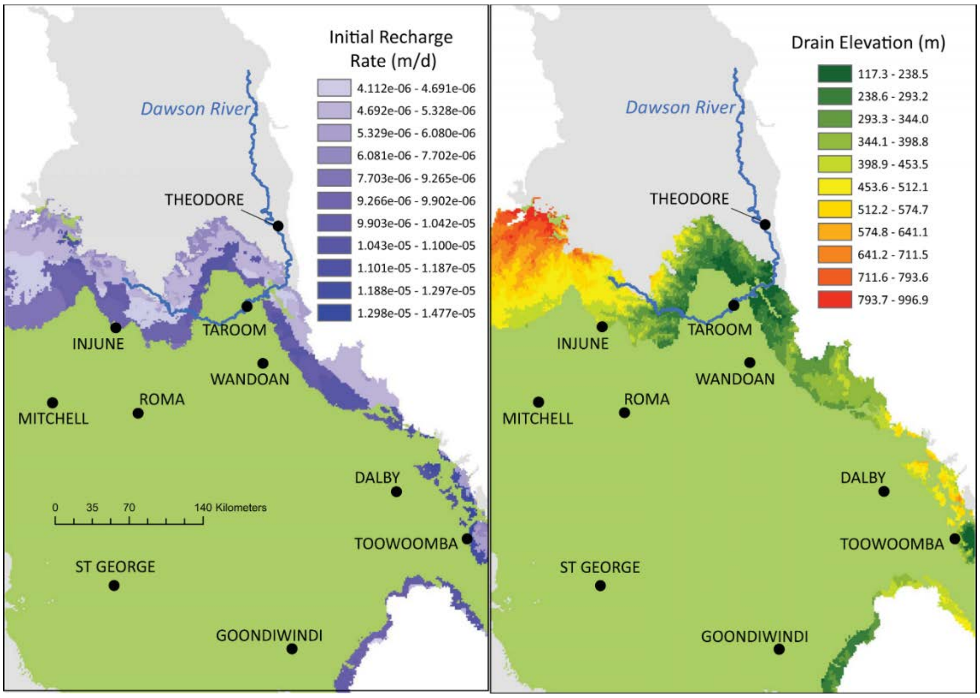

Figure 2.5: Initial estimates of recharge rates and the elevations used in OGIA's current Surat CMA model.

Model Parameterisation and Observation Data

The current Surat CMA model version, the basis for the present study, was calibrated by OGIA using the PEST software suite (*Doherty*, 2016a, 2016b). The calibration process for this model consisted of over 7,000 parameters and 16,0s00 observations (*OGIA*, 2016c). Hydraulic head measurements comprised the majority of the observation dataset and consisted of measurements that represent pre-development steady-state conditions and transient post-CSG conditions. Other measurement types consisted of flux constraints (e.g., enforcing a zero-flux exchange between the Surat Basin and the GAB in the west, Condamine water flux exchange, etc.), vertical head differences or gradients, water saturation conditions in coal seams, etc. The majority of the spatial parameterisation was conducted via pilot point interpolation, which included hydraulic conductivity, vertical anisotropy, Condamine Alluvium hydraulic properties, general-head boundary parameters, and coal cleat storage. Other parameters consisted of recharge multipliers, fault conductance, and additional parameters required for the coal measures, e.g., the ratio of the dual domain transfer flow rate to upscaled vertical hydraulic conductivity.

Due to the high degree of parameterisation relative to the information content in the observation dataset, the inverse problem was ill-posed. Therefore, regularisation was applied using two strategies, subspace methods and Tikhonov regularisation. The subspace method projects the inverse problem onto a subspace of the parameter vector space, i.e., the so-called "solution space". Tikhonov regularisation is an approximate Bayesian estimation approach for nonlinear inverse problems, where prior information is imposed on the parameter values. Tikhonov prior information, or constraints, consisted of (1) homogeneity assumptions along GHB boundaries and some interlayer properties such as the Brooks-Corey exponent, a parameter for the relationship between hydraulic conductivity and moisture content in the unsaturated zone, for example, and (2) initial values assigned to each of the remaining parameters.

The calibration results show an overall reasonable agreement with observed data (see *OGIA*, 2016c for details). The estimated hydraulic conductivity is, in general, higher in the Precipice Sandstone than in the Hutton Sandstone (Figures 6 and 7). However, due to the fact that the inverse problem is overparameterised, the calibrated parameter set is not unique. To the best of our knowledge, OGIA has not addressed this issue through the formal quantification of parameter and/or predictive uncertainty, e.g., via the Null-Space Monte Carlo method. Therefore, in this study, we focus on a single parameter set issued by OGIA as outlined in *OGIA* (2016c). There are some potentially significant limitations to this, which are outlined in subsequent sections.

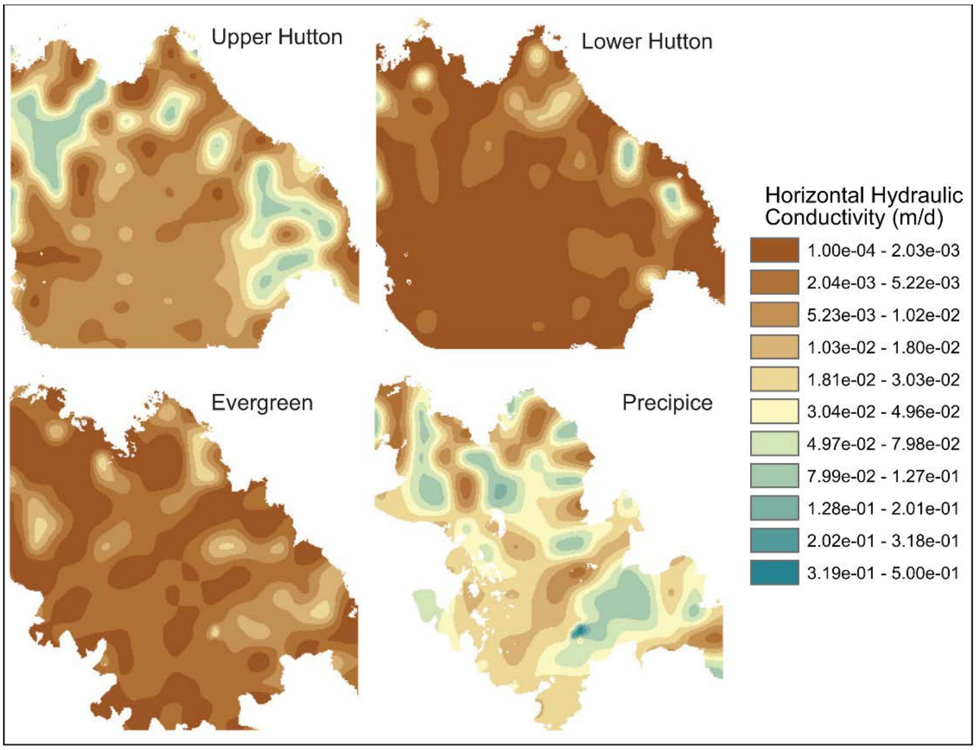

Figure 2.6: Horizontal hydraulic conductivity field estimated by OGIA for the Surat CMA model. The high density of the pilot points is evident in these distributions.

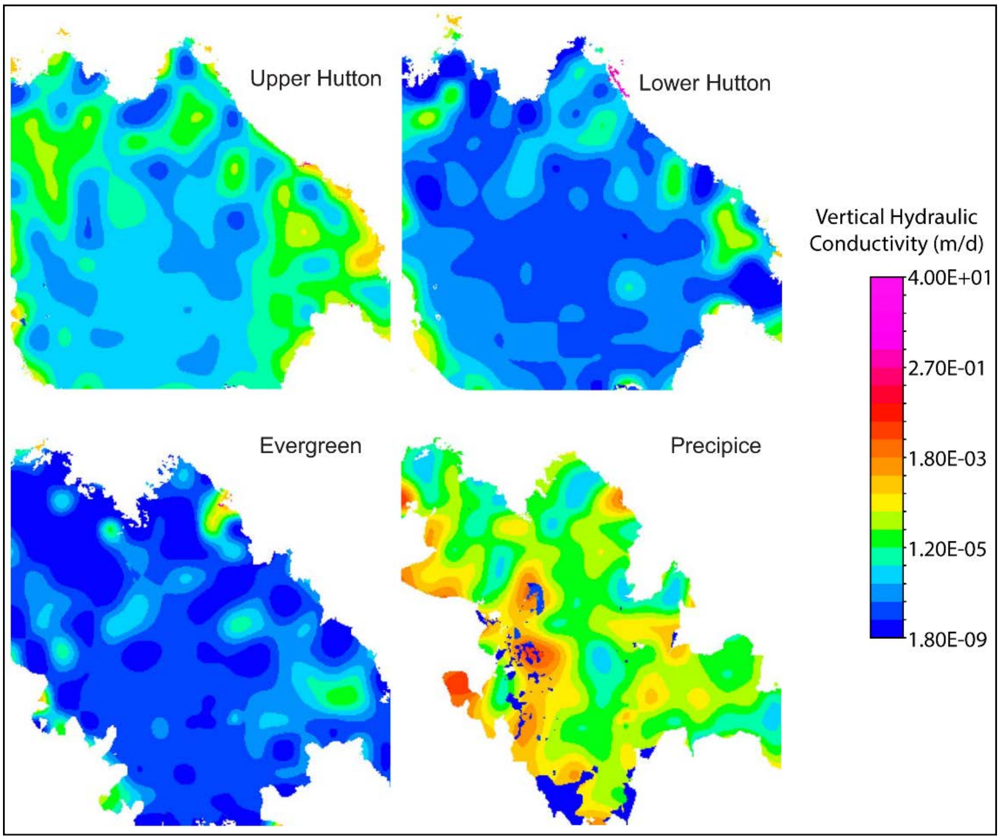

Figure 2.7: Vertical hydraulic conductivity field estimated by OGIA for the Surat CMA model. The high density of the pilot points is evident in these distributions.

2.3.2 GROUNDWATER FLOW AND REACTIVE TRANSPORT MODEL DEVELOPMENT

In the case of the Surat CMA, the groundwater flow model developed by *OGIA* (2016c) is the best tool for the establishment of an accurate flow field simulator. However, since the unstructured-grid version of MODFLOW was employed as OGIA's modelling platform, the direct use of the resulting computed flow fields for the solute transport simulations with MT3DMS (*Zheng and Wang*, 1999) was not feasible. Therefore, an appropriate workflow had to be developed to facilitate the use of OGIA's Surat CMA model, and associated surrogate models, as a basis for simulating the reactive transport of multiple environmental tracers.

MODFLOW-USG allows for unstructured grid usage in groundwater flow modelling. While this provides significant advantages for flow model simulations, as discussed previously, the employed transport simulator MT3DMS requires the definition of rectilinear, structured model grids. This is mostly due to practical considerations in the spatial construction of the finite difference or mixed Eulerian-Lagrangian equations. In this study, we take advantage of the fact that the Surat CMA is constructed as a rectilinear model and the only "unstructured" model features utilised in this model are (i) the pinching-out of model layers and (ii) the vertical connections induced along faults. Furthermore, the severity of these unstructured features is less pronounced from the Hutton Sandstone down to the Precipice Sandstone. There are, in fact, a number of model cells that pinch-out in the Precipice Sandstone but since this is the deepest layer of interest, this pinching-out has no impact if transport within the deeper Bowen Basin is not simulated. Therefore, it is possible to reconstruct a surrogate (sub)model of the Surat CMA model using a rectilinear, structured grid that is compatible with the requirements of the MT3DMS transport simulator.

Extracting the Flow Field for the Hutton Sandstone, Evergreen Formation and Precipice Sandstone Aquifers

The approximate simulation of the flow field from the Hutton Sandstone down to the Precipice Sandstone with a rectilinear, structured grid is a two-step process. The first step is to simply execute the full Surat CMA model as developed by OGIA. The second step is to extract relevant hydraulic simulation output to develop a separate groundwater flow model for the Hutton Sandstone down to the Precipice Sandstone. This separate model, which only corresponds to the 1947 steady-state simulation of the Surat CMA model, will be referred to as the *surrogate flow model* from here on in this report.

The surrogate flow model employs the exact same discretisation and extent as the Surat CMA model for the Hutton, Evergreen and Precipice model layers (Figure 2.4). Additionally, since the outcrop areas for these aquifers are not connected to any model layers above them (i.e., the layers are expressed at land surface), the exact same recharge/drain boundary conditions can be applied in these areas (Figure 2.5). Therefore, the only boundaries for the surrogate flow model that differ from the Surat CMA model are the vertical connections to the aquifers/aquitards above the Hutton Sandstone and those below the Precipice Sandstone. In the surrogate flow model, these boundaries are simulated as connections with constant-head model cells, where the prescribed hydraulic head is set to the values resulting from the simulation of the full Surat CMA model. That is, a model layer is added above the Hutton Sandstone which is comprised entirely of constant-head model cells whose prescribed values are set to the simulated results of the full Surat CMA model; a similar model layer is added below the Precipice Sandstone to account for vertical connections in this direction. The surrogate flow model is subsequently simulated at steady-state using MODFLOW-2005. Figure 2.8 illustrates this procedure.

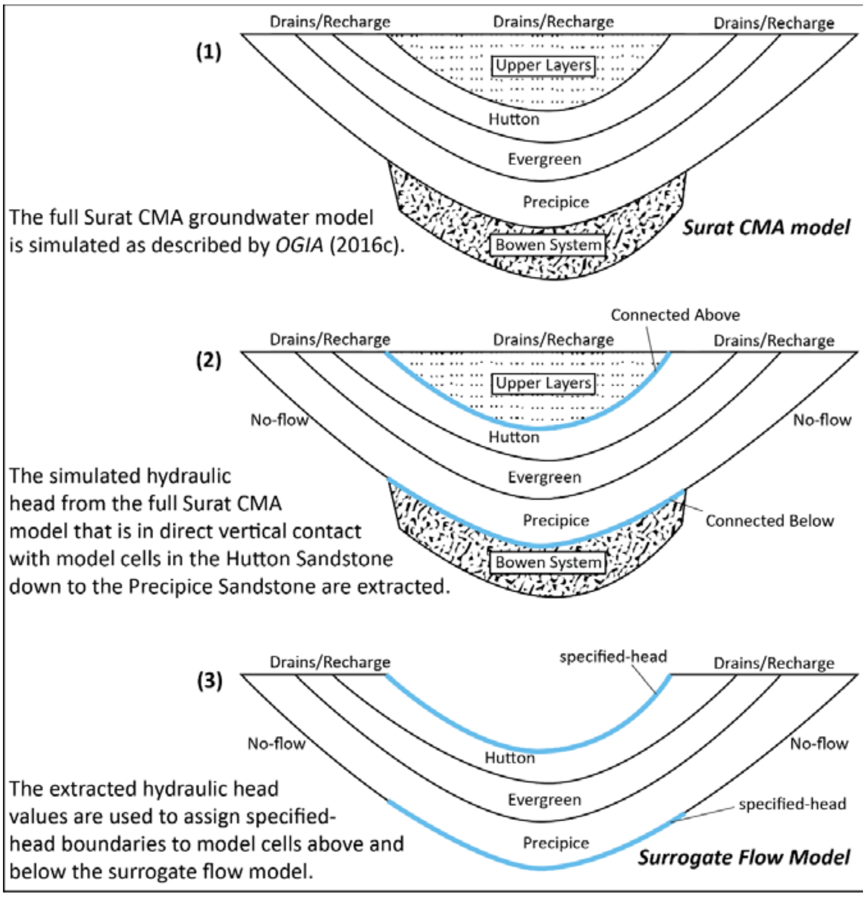

Figure 2.8: Illustration of the methodology used in this study to convert the flow field from the rectilinear MODFLOW-USG Surat CMA groundwater flow model into a rectilinear but structured surrogate flow field for only the Hutton Sandstone down to the Precipice Sandstone aquifers. The resulting surrogate flow model is simulated with MODFLOW-2005 with the same discretisation and recharge/drain boundary conditions as the 1947 steady-state Surat CMA model simulation.

While this methodology may seem straightforward, care must be taken when extracting the simulated hydraulic head from the Surat CMA model due to the potential for pinched-out layers. That is, the hydraulic head for a given model cell in the Upper Hutton Sandstone (i.e., layer 18) may not necessarily be connected with the next layer up, the Durabilla Formation (i.e., layer 17). Similarly, the downward connections to the Bowen Basin are complex; Figure 2.9 depicts the extent of the constant-head cells by model layer for the surrogate flow model, which has six model layers (layers 1 and 6 represent the most upward and downward connections, respectively).

For some areas in the south-eastern region of the domain, the Upper Hutton is in direct contact with layer 1, the alluvium and basalt (including Main Range Volcanics), indicating that layers 2-17 are non-existent in these regions; similarly, in the south-western portion of the Upper Hutton, layer 17 is pinched out and the Upper Hutton is in direct connection with layer 16, the lower Walloon Coal Measures (Figure 2.9). There are some other upward connections present in the Upper Hutton including the Upper Springbrook Sandstone (layer 9) and the Upper Cretaceous/Cenozoic sediments (layer 2). There is also a small upward connection to shallower layers along a fault line in the north central region (a portion of the Hutton-Wallumbilla Fault system). Since multiple vertical connections in a single direction (upward or downward) are not allowed in structured grids, the overall connectivity of the fault system cannot be simulated in the surrogate flow model; this may potentially produce some small errors.

The Precipice Sandstone pinches-out in many locations as depicted in Figure 2.9. Therefore, in these regions the Evergreen Formation has a direct connection with the model layers of the Bowen Basin (i.e., layers 22-32 of the Surat CMA model). For each of these locations, a constant-head cell is required within the Precipice Sandstone (layer 5 of the surrogate flow model). This presents a relatively small source of error since in the Surat CMA model, the deeper Bowen Basin layers do not connect laterally with the

Precipice Sandstone. However, since both the magnitude of the induced error and the number of model cells affected are small, this likely has little overall impact on system dynamics (Figure 2.10). The Precipice Sandstone, where active, directly connects with the Bowen Basin below, with the layer number indicating which layers in the Bowen Basin are pinched-out; it is apparent that several of the Bowen Basin model layers pinch-out along the Mimosa Syncline (Figure 2.9).

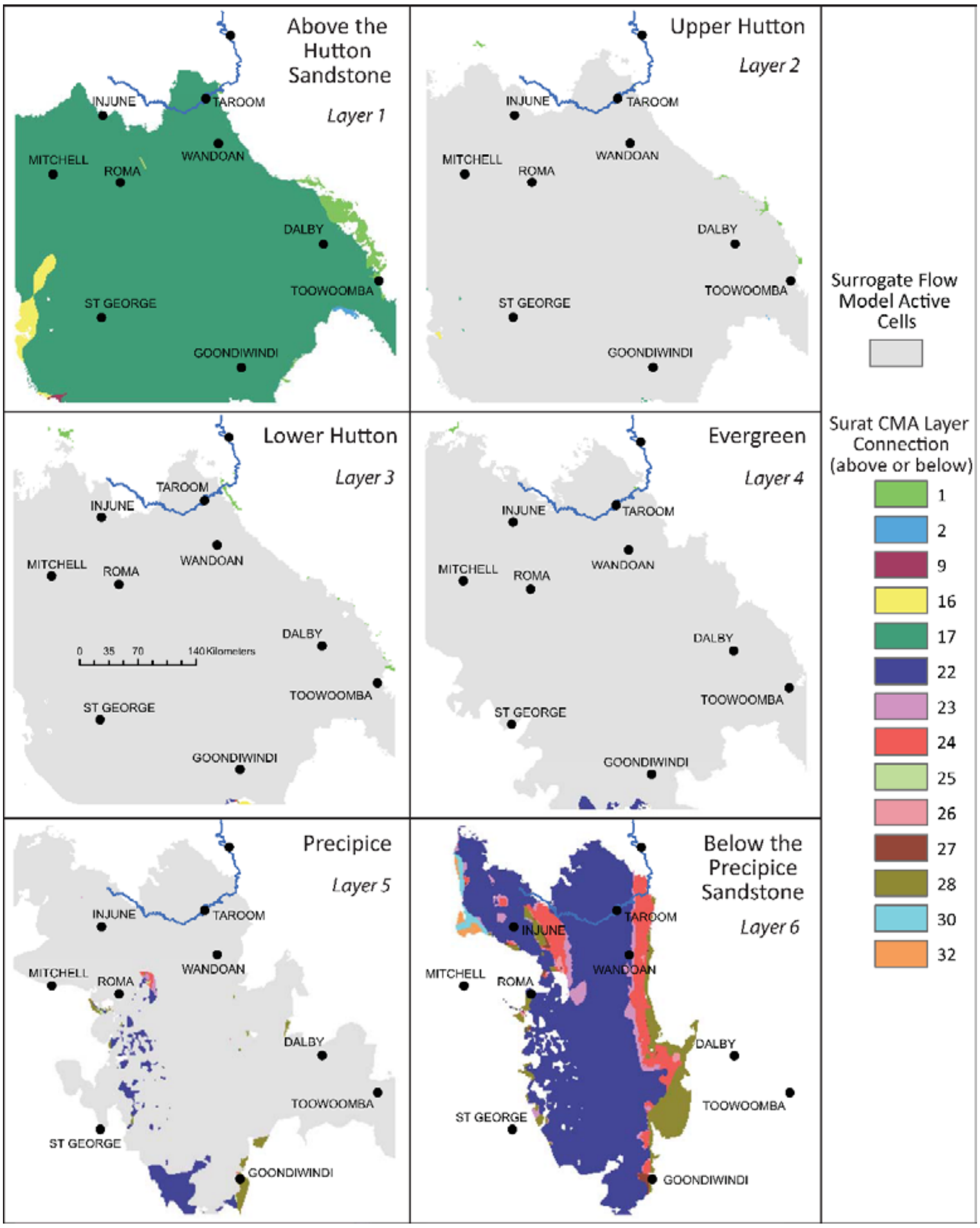

Figure 2.9: Vertical connections used to define constant-head cells in the six-layer surrogate flow model. Grey active areas indicate regions where the surrogate flow model simulates groundwater flow. The layers above the Hutton Sandstone and below the Precipice Sandstone are entirely comprised of constant-head cells. The active layers in between still contain some vertical connections (and hence, constant-head cells) to layers above the Hutton Sandstone or below the Precipice Sandstone due to other layers not being active in these regions. This feature is most pronounced in the Precipice Sandstone where numerous cells represent a connection between the Evergreen Formation and the layers beneath the Precipice Sandstone (where the Precipice Sandstone is inactive).

Once the Surat CMA model is executed (again, for the 1947 steady-state simulation), the hydraulic head data, corresponding to the coloured model cells depicted in Figure 2.9, are extracted and used as constant-head cells in the surrogate flow model. Subsequently, the surrogate flow model is executed within MODFLOW-2005 using a rectilinear, structured model grid. Using the single calibrated parameter set provided by *OGIA* (2016c), this process was conducted to verify that the simulated results of the surrogate flow model agree with those of the Surat CMA model, which indeed showed generally good agreement

(Figure 2.10). During the execution of the surrogate flow model, the flow field required as input for the subsequent MT3DMS simulation can be automatically generated. With this workflow in place, the incorporation of environmental tracers into the calibration process of the Surat CMA is now possible.

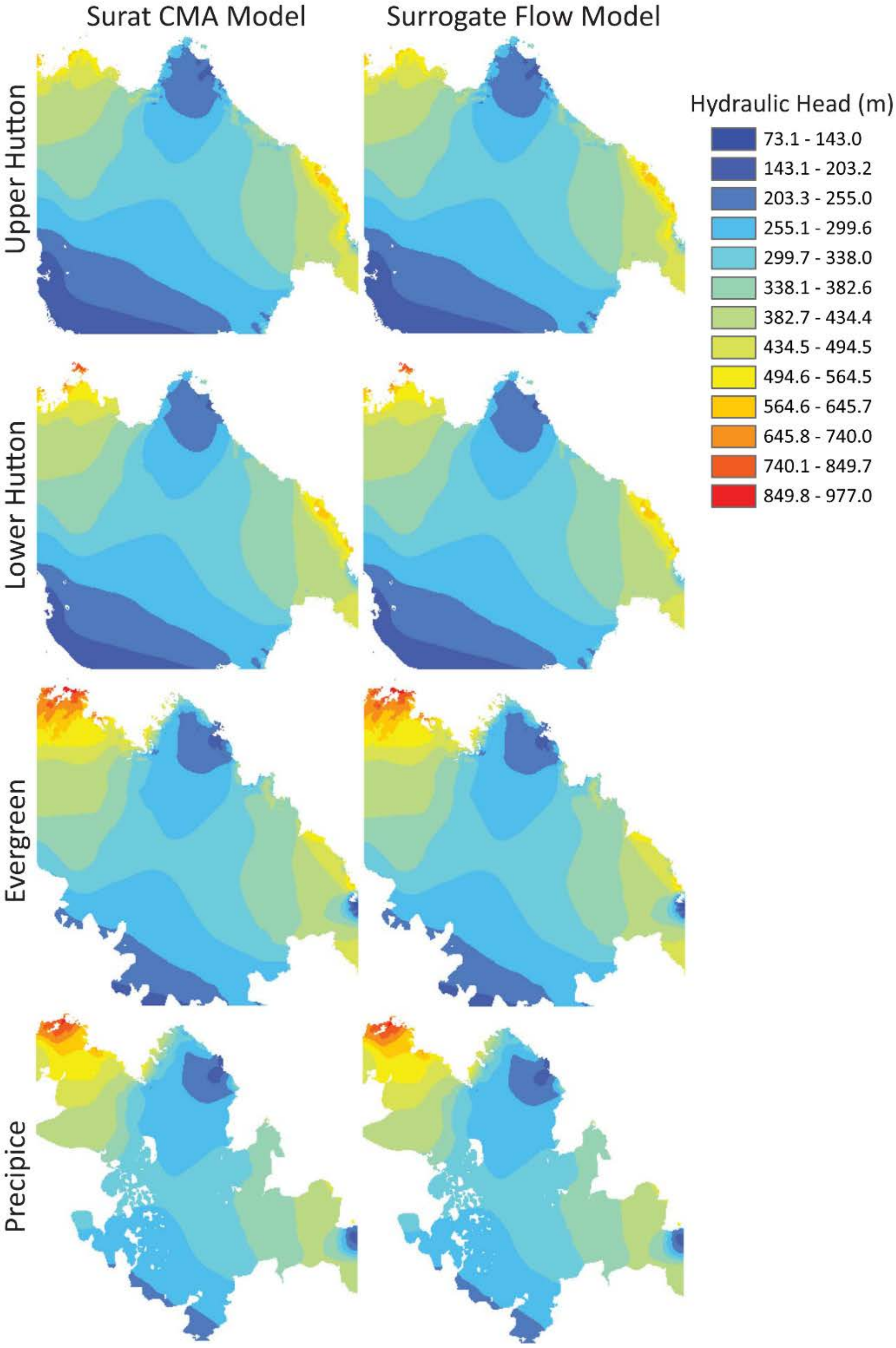

Figure 2.10: Comparison between the simulated hydraulic head distributions of the Surat CMA and the surrogate flow model for the 1947 steady-state simulation using the single calibrated parameter set provided by OGIA (2016c).

Environmental Tracers for Old Groundwater

Environmental tracers are produced naturally either within the atmosphere (e.g., ^{14}C, ^{36}Cl, etc.) or within the subsurface (e.g., ^{4}He, ^{36}Cl, etc.). Once they are recharged and/or dissolved within the groundwater, they are transported through the aquifer system via advective and dispersive-diffusive mechanisms. Using knowledge about how tracers are produced and how they enter the groundwater system, along with measured concentrations from groundwater samples, hydrologists have in the past inferred qualitative or semi-quantitative information about the flow paths and residence times of a particular groundwater system. In most cases environmental tracer concentrations were converted to (apparent) groundwater ages before being used to support the characterisation of groundwater flow system (*Suckow*, 2014). This conversion is based on the known physico-chemical behaviour of the considered environmental tracer. For example, some radioactive tracers such as ^{14}C undergo decay under well-known (first-order) decay rates as they move through the groundwater system. Inferring groundwater ages using these radioactive tracers requires (1) knowledge or assumptions of the abundance of each tracer upon groundwater recharge (C_0), i.e., at the time the tracer enters the saturated zone of the groundwater system (2) the decay rate (λ) or half-life of the respective tracer, and (3) the observed concentration of the tracers (C). In this case the (apparent) groundwater age can be computed from:

$$C = C_0 e^{-\lambda t} \Rightarrow age = -\frac{1}{\lambda} ln\left(\frac{C}{C_0}\right) \tag{1}$$

However, inferring an apparent groundwater age from a tracer sample in this way relies on many simplifying assumptions and thus contains numerous uncertainties. Some of the factors that often render such an analysis unreliable include, geochemical influences, multiple sources (e.g., both atmospheric and geologic), mixing of old and young groundwaters, dispersion, diffusion into or out of aquitards, etc. As a result, *Love et al.* (2000), for example, found that estimating flow velocities using ^{36}Cl was more precise than groundwater age due to complicating factors including, "dead" Cl diffusion from aquitards and the difficulty associated with quantifying steady state *in situ* production. However, many of these "complicating factors" such as mixing/dispersion etc., can be accounted for through their explicit consideration in numerical reactive transport models.

In this study, we use tracer concentrations directly within a numerical modelling framework to make quantitative conclusions about flow paths, recharge rates, and residence times. This is possible because numerical flow and transport models intrinsically account for many of the uncertainties incurred during the interpretation of tracer concentrations including, multiple sources, dispersion, diffusion into or out of aquitards, and mixing of old and young groundwaters. This study is primarily focussed on the simulation and information content associated with ^{36}Cl and ^{14}C. Both ^{36}Cl and ^{14}C are produced in the atmosphere and enter the groundwater system via rainfall/recharge. ^{36}Cl can be produced in the subsurface primarily via the decay chains of uranium and thorium. ^{36}Cl and ^{14}C are radioactive tracers that undergo first-order decay; their half-lives are about 301,000 and 5,730 years, respectively. ^{36}Cl is an ideal tracer for groundwaters that are between 100,000 and 1 million years old, and ^{14}C is an ideal tracer for groundwaters that are between 2,000 and 40,000 years old. However, concentrations of both tracers can be affected by physical and/or chemical processes that render the direct use of Equation 1 completely unreliable.

Transport model for ^{36}Cl

Perhaps the most significant complication associated with the use of ^{36}Cl is that it can be produced in the subsurface from stable ^{35}Cl atoms via the decay chains of uranium and thorium. This process is referred to as neutron activation (*Park et al.*, 2002),

$$^{35}\mathrm{Cl} + {}^{1}_{0}\mathrm{n} \longrightarrow {}^{36}\mathrm{Cl}$$

The production of ^{36}Cl is therefore dependent on the abundance of stable ^{35}Cl ($\chi_{35} = 0.75775$), the total Cl concentration (C_{Cl}), the neutron flux (Φ_n), which is a function of the presence of uranium and thorium, the porosity (ϕ), and finally the neutron capture cross section of ^{35}Cl ($\sigma_{35} = 43.74 \times 10^{-24}$). The production rate of ^{36}Cl is assumed to be zeroth-order and simply a multiplication of these components (*Park et al.*, 2002),

$$P_{36} = \Phi_n \phi \chi_{35} \sigma_{35} C_{Cl} \tag{2}$$

The production rate of ^{36}Cl is therefore a spatially distributed phenomena. However, in this study it was assumed that the production rate is spatially homogeneous. This assumption is reasonable because the observed ^{36}Cl abundance (i.e., $^{36}Cl/Cl$) appears to have reached a relatively constant value at some distance from the outcrop areas. This relatively constant value is most likely the result of an equilibrium between radioactive decay and production of ^{36}Cl, often referred to as secular equilibrium. It can be shown that the secular equilibrium for ^{36}Cl abundance (R_{se}^{36}) can be simply be written as the ratio of the ^{36}Cl production rate (excluding the concentration of Cl) and the decay rate,

$$R_{se}^{36} = \frac{\Phi_n \phi \chi_{35} \sigma_{35}}{\lambda} \quad (3)$$

In this study, the ^{36}Cl abundance, i.e., R^{36}, is used as the state variable. This assumes that the Cl entering the system with the ^{36}Cl migrates along the same flow paths as ^{36}Cl and that there is no "dead" Cl that can influence the abundance measurements. This assumption is likely valid since *Suckow et al.* (2016; 2018) indicated that dead Cl does not play a significant role in the Hutton and Precipice Sandstones.

The original version of the MT3DMS code is limited to the simulation of either 0th-order or 1st-oder chemical decay or production processes and therefore unable to simulate the simultaneous decay and production of ^{36}Cl. Therefore, the source code of MT3DMS had to be accordingly modified and tested as part of this study. The revised code now allows to compute a steady-state transport solution for arbitrary combinations of these two mechanisms.

Transport model for ^{14}C

The abundance of ^{14}C in aquifers and its use as an environmental tracer is affected by numerous biogeochemical processes that remain uncaptured by the use of Equation 1. Potential complications or errors arise where dissolution, precipitation, or recrystallisation of carbonate materials occurs. Furthermore, the oxidation of either dissolved or sedimentary organic carbon may affect the abundance of ^{14}C. For example, *Salmon et al.* (2015) demonstrated through numerical two-dimensional reactive transport simulations the impact of some of these processes on the inference of apparent groundwater ages and found them to be quite significant in some cases. Some of these biogeochemical factors may be relevant in the Surat Basin, e.g., the potential downward migration of dissolved organic carbon from the coal measures above the Hutton Sandstone, or the oxidation of methane migrating from below into the aquifers. In these examples, "dead" C (total C with no ^{14}C present) is transported and mixed with the measured groundwater that contains ^{14}C, diluting the ratio of ^{14}C/C, rendering the measured sample non-representative of true groundwater residence times. However, the explicit simulation of most of these factors remains at this stage intractable for regional-scale three-dimensional groundwater models. Therefore, only the first-order decay process of ^{14}C could be considered in this study.

Reactive Transport Model for the Surat CMA

The reactive transport simulations considered in this study, for all tracers, employ the simplifying assumption that both flow and transport can be approximated by steady state flow and transport simulations. This assumes that the flow field has not changed over the entire computed residence time and that the tracer distributions are stationary in time. Both assumptions clearly provide some source of error. However, as already mentioned previously, the ^{36}Cl observations appear to reach secular equilibrium in the central Hutton Sandstone, which indicates that in these regions the tracers are in fact stationary over the relevant time scale. Additionally, due to the depth of the aquifer systems and the relatively short duration of groundwater pumping (compared to the time scale of radioactive decay of ^{14}C and ^{36}Cl), anthropogenic influences are assumed to have a negligible influence on current day tracer distributions, as mentioned previously.

The atmospheric source of ^{36}Cl and ^{14}C is assumed to enter the groundwater system via recharge from precipitation. Therefore, an appropriate concentration, or abundance, must be assigned to incoming water at the outcrops of the Evergreen Formation and the Hutton and Precipice Sandstone for these tracers (Figure 2.4). Since the outcrop areas contain both recharge and discharge (due to drains rejecting recharge), a specified concentration was only assigned to the incoming, or net recharge, waters. This is accomplished using a constant-concentration source in MT3DMS in the outcrop areas. The incoming ^{36}Cl/Cl abundance was assumed to be 120×10^{-15}, as previously suggested by *Suckow et al.* (2016; 2018), while the incoming ^{14}C/C abundance was assumed to be 100 percent modern carbon (pmc). Since there is some potential for groundwater to migrate upward from the deeper Bowen Basin, any incoming groundwater from below was assigned a ^{36}Cl abundance consistent with what the bulk of the ^{36}Cl/Cl data in the interior of the Surat Basin indicates and is at secular equilibrium, about 15×10^{-15}. The incoming groundwater from below the Precipice Sandstone was given a ^{14}C abundance of 0 pmc. The longitudinal dispersivity was set to 100 m for all simulations due to long transport distances, with a horizontal transverse dispersivity of

10 m and a vertical transverse dispersivity of 1 m. The diffusion coefficient for ^{36}Cl and ^{14}C was set to 1.08×10^{-4} m²/d (*Cussler*, 2009) and 1.12×10^{-4} m²/d (*Cook and Herzceg*, 2000), respectively.

Preliminary simulations showed some counterintuitive results in the south-eastern portion of the model domain. The results in these regions were "spotty" due to a lack of incoming tracers where the outcrops are not expressed at land surface. This is likely due to the fact that the Upper Hutton Sandstone is overlain by alluvium and basalt in this region, i.e., layer 17 is connected to layer 1 above (Figure 2.9). This indicates that the overall thickness of the porous medium above the Upper Hutton is relatively thin in these regions and that ^{36}Cl and ^{14}C abundances associated with water entering the Upper Hutton Sandstone here may not differ much from the atmospheric levels. Therefore, atmospheric abundances were also assigned to incoming water entering the Upper Hutton Sandstone where it is in contact with the alluvium and basalt above (i.e., layer 1). This essentially "fills in the gaps" along the outcrop areas to produce a more intuitive shape and distribution (Figure 2.11). Although this improves the simulation of the tracers in these areas, some spotty distributions still persist, which are likely due to strong upward fluxes in this region as simulated by the Surat CMA model.

Figure 2.11: Overall outcrop areas where atmospheric abundance of associated tracers are set to constant-concentration for incoming water. The green regions comprise the overall outcrop areas considered for the aquifers of interest in this study (Figure 2.4). The blue regions represent the areas where relatively thin alluvium and basalt aquifers overlay the Upper Hutton Sandstone aquifer. These blue regions are also assigned constant-concentrations of incoming waters at atmospheric levels.

2.3.3 MODEL CALIBRATION

The calibration process involved the estimation of both flow and transport parameters using a calibration dataset consisting of hydraulic heads as well as ^{36}Cl and ^{14}C abundances. The parameterisation employed in the Surat CMA model by OGIA is complex and involves thousands of pilot points (*OGIA*, 2016c). However, their calibration timeline also included both a secondary steady-state, and a transient simulation with thousands of associated hydraulic head measurements. At the time of this study, it was not feasible to utilise these additional simulations and overall observation dataset developed by OGIA. However, OGIA has provided the hydraulic head data corresponding to the 1947 steady-state period of their model.

As a result of having fewer hydraulic head observation data, the pilot point interpolation scheme adopted in this study utilises far fewer parameters (i.e., pilot points) than that employed by *OGIA* (2016c). In this study, seven pilot points are used for the spatial parameterisation of horizontal/vertical hydraulic conductivity and porosity for each model layer (Figure 2.12). The vertical hydraulic conductivity of the Upper Hutton Sandstone was kept fixed at the distribution provide by *OGIA* (2016c) to alleviate potential correlation in vertical conductance calculations within the aquifers of interest.

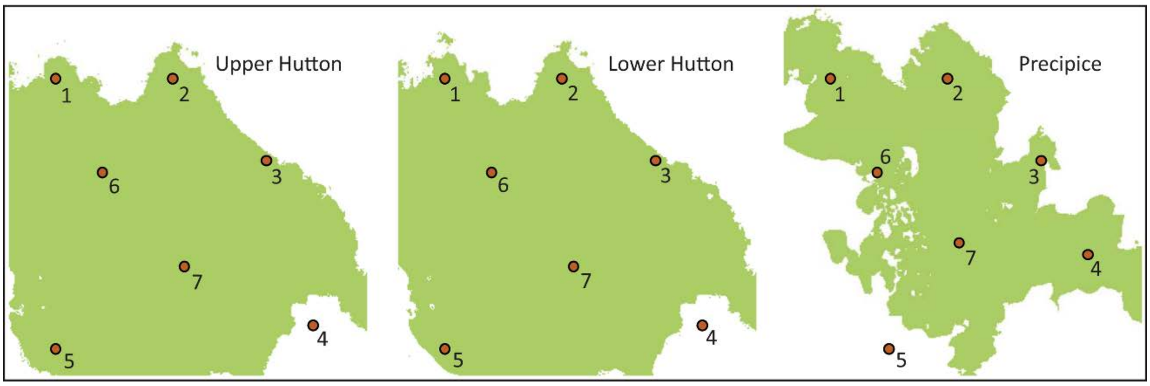

Figure 2.12: Pilot point locations used to parameterise spatial distributions of hydraulic conductivity and porosity. The pilot point locations in the Upper and Lower Hutton Sandstone are the same; the locations have been adjusted slightly in the Precipice Sandstone due to aquifer geometry. The Evergreen Formation is assumed to be homogeneous.

Additional parameters consisted of recharge adjustment factors and the ^{36}Cl production rate. The initial recharge estimates are assumed to be uncertain, and therefore a multiplier is applied to adjust the entire recharge distribution for each of the four outcrop areas. This assumes that the relative distributions are reasonably accurate, but the overall magnitude may not be (*OGIA*, 2016c). Therefore, there are a total of 64 parameters considered in this study, 22 pilot points for horizontal hydraulic conductivity, 15 for vertical hydraulic conductivity, 22 for porosity, 4 recharge multipliers, and the ^{36}Cl production rate. This study provides the first regional estimates for porosity, as this was not estimated by OGIA (2016c). For future work, permeability estimates could be improved by examining porosity-permeability structures.

Although the number of parameters implemented in this study is much smaller than that by *OGIA* (2016c), the inverse problem was nevertheless under-determined. Therefore, Tikhonov regularisation was employed to impose prior information consisting of the assumption of spatial homogeneity, i.e., regularisation constraints were set up such that the pilot point parameters within each layer were equal to one another. The final estimated parameters therefore only deviate from the others if the observation data requires it.

The hydraulic head dataset representing 1947 steady-state conditions contained 498 measurements located throughout the entire model domain; only 59 of which are perforated in the Evergreen Formation and the Hutton and Precipice Sandstone aquifers (*OGIA*, 2016c) (Figure 2.13). The observed ^{36}Cl and ^{14}C abundances were obtained from previous sampling campaigns (*Ransley and Smerdon*, 2012; *Feitz et al.*, 2014) and both the previous and current GISERA projects (*Suckow et al.* 2016; 2018) and are depicted in Figures 14 and 15 (among others). There are a total of 114 ^{14}C and 97 ^{36}Cl measurements used in the calibration process resulting in an overall total of 709 field observations. The weights assigned to each observation type (i.e., hydraulic head, ^{14}C and ^{36}Cl abundances) were based on (1) the relative magnitude of the observation type (2) the associated relative measurement/conceptual errors, and (3) the number of observations within the group. This resulted in a relative contribution from each observation type to the overall least-squares objective function that is commensurate with these factors.

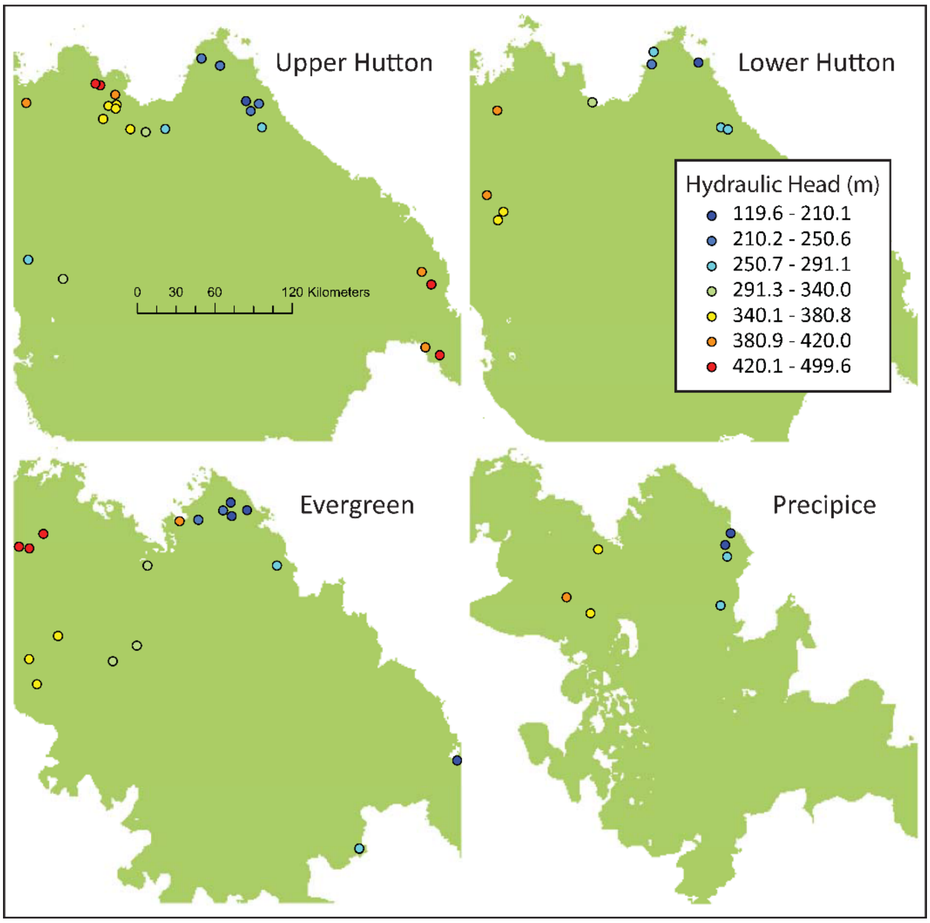

Figure 2.13: Observed 1947 hydraulic head data in the Evergreen Formation and Hutton and Precipice Sandstone aquifers (*OGIA*, 2016c).

Observations of tracer abundances where generally classified into being in either the Hutton or the Precipice Sandstone. This assumes that there are no samples that represent the Evergreen Formation. Since the Hutton Sandstone was divided into two model layers (*OGIA*, 2016c), the perforated interval for each bore in the Hutton Sandstone, where tracers were sampled, must be considered. This is important for the calibration process as tracer concentrations can differ significantly between model layers. This is especially true near the outcrop areas. The hydrostratigraphic formation at the screened interval was independently confirmed for each bore using bore construction details and three-dimensional geological models as outlined by *Raiber and Suckow* (2017). Where perforated intervals either, (1) were unknown, or (2) suggested that the bore was completed in both layers, or (3) suggested that the bore was completed above or below the aquifers of interest based on numerical model layer elevations, a single layer was chosen as the representative layer based on surrounding data and expert knowledge.

Model parameters for various setups were estimated by PEST (Appendix A). Each “model” within a PEST run consisted of a series of steps to execute the following overall workflow,

1. Conduct pilot point interpolation for horizontal, vertical hydraulic conductivity and porosity.
2. Run scripts to insert hydraulic parameter fields into the Surat CMA model (MODFLOW-USG) for the Hutton Sandstone down to the Precipice Sandstone layers.
3. Run scripts to apply recharge adjustment factors.
4. Execute the Surat CMA model (MODFLOW-USG).
5. Extract hydraulic head from Surat CMA model output corresponding to the constant-head boundaries of the surrogate flow model (Figure 2.9).

6. Using these boundary conditions, along with the hydraulic and recharge parameter fields, execute the surrogate flow model (MODFLOW-2005).
7. Using the groundwater flow field from the surrogate flow model and the porosity parameter fields, execute the reactive transport model (modified MT3DMS) for both ^{36}Cl and ^{14}C.
8. Run scripts for extracting the model-simulated equivalents of the hydraulic head observations from the Surat CMA directly (i.e., not from the surrogate flow model).
9. Run scripts for extracting the model-simulated equivalents of the tracer abundance observations from the reactive transport model.

The above process was conducted each time PEST tested a particular parameter set. The overall runtime of the above process was about 10-20 min.

The above discussed simulation and calibration workflows were developed to successively improve the conceptualisation and calibration and of the Hutton and Precipice Sandstone aquifers within the Surat CMA. Initially, the flow field resulting from the single calibrated parameter set provided by *OGIA* (2016c) was used to simulate the reactive transport of the environmental tracers ^{36}Cl and ^{14}C. However, these initial simulations provided an inadequate representation of the environmental tracer distributions. Therefore, the model was re-calibrated, for the Hutton down to the Precipice Sandstone aquifers only.

3 Results and Discussion

3.1 Environmental Tracer Simulation for Unmodified Surat CMA Model Parameterisation

The Surat CMA model was executed using the single calibrated parameter set provided by *OGIA* (2016c) as described in Section 2.3.1. As explained by *OGIA* (2016c), the Surat CMA model reasonably reproduces the observed hydraulic head distribution in the aquifers of interest; see *OGIA* (2016c) for detailed results. Using the flow field from this simulation, with a reasonable, uniform value for porosity of 0.15, and a ^{36}Cl production rate of 6.3×10^{-8}/d, Figures 14 and 15 depict the simulated ^{36}Cl and ^{14}C distributions using the surrogate flow field described previously with the hydraulic parameters provided by OGIA. It is immediately evident that the hydraulic parameters, and perhaps porosity and ^{36}Cl production rate, would need to be refined and revised in order to produce a better agreement between the model simulated and the observed tracer concentrations. The observed ^{36}Cl data in the Precipice Sandstone are less reliable than those in the Hutton Sandstone (see *Suckow et al.* (2016; 2018) for further details); nevertheless, it is clear that higher permeabilities will be required to allow ^{36}Cl to migrate faster within this layer such that observed ^{36}Cl concentrations further away from recharge areas remain no longer underestimated. Similarly, the ^{36}Cl results in the Hutton Sandstone also indicate that higher permeabilities are likely required for this layer, especially in the northern regions. A secular equilibrium of 10×10^{-15} is reached for ^{36}Cl abundance throughout the central portion of the basin, which is in good agreement with most of the data in this area. Therefore, it is clear that ^{36}Cl data collected in the centre of the basin are likely to be more useful for determining the ^{36}Cl production rate rather than for inferring groundwater flow paths or residence times. Therefore, the groundwater in these central regions is likely to be millions of years old.

Due to the fact that the groundwater appears to be very old in the Surat Basin, perhaps on the order of millions of years in the central regions of the Hutton Sandstone, the collected ^{14}C data, while important to be sampled in the first place, do not appear to provide any significant constraints for regional model calibration, except possibly in the Precipice Sandstone. This is due to the fact that both the simulated and the observed ^{14}C concentrations approach 0 pmc only a few model cells inward from the outcrop area, primarily in the Hutton Sandstone. This data was nevertheless included in the re-calibration of the model. However, from here onward in this report, the discussion will be focussed primarily on the ^{36}Cl results in the Hutton Sandstone, and the ^{14}C results in the Precipice Sandstone aquifers.

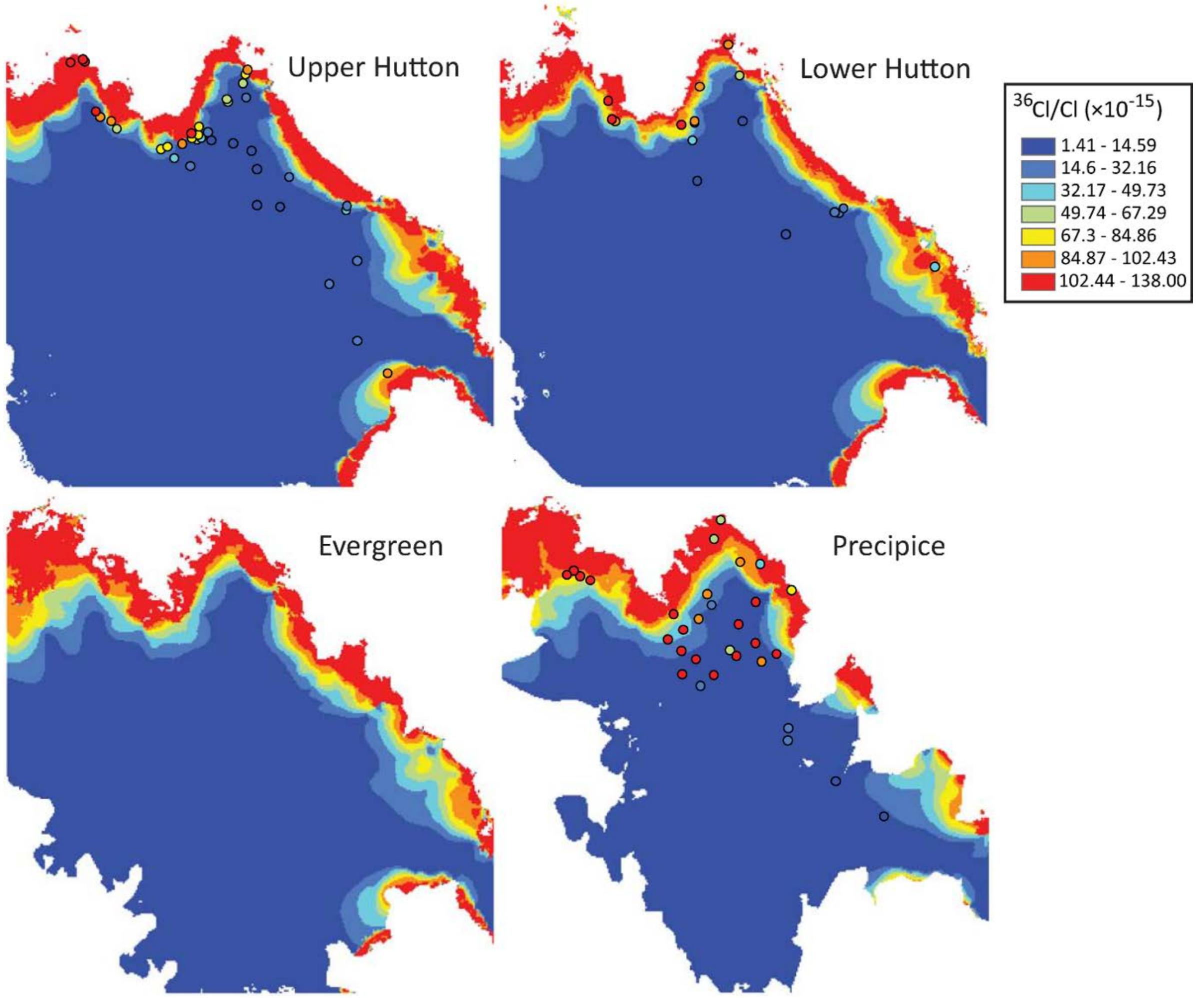

Figure 3.1: Initial simulation of (and observed) ^{36}Cl abundances for the Hutton down to the Precipice Sandstone aquifers using the single calibrated parameter set provided by OGIA (2016c).

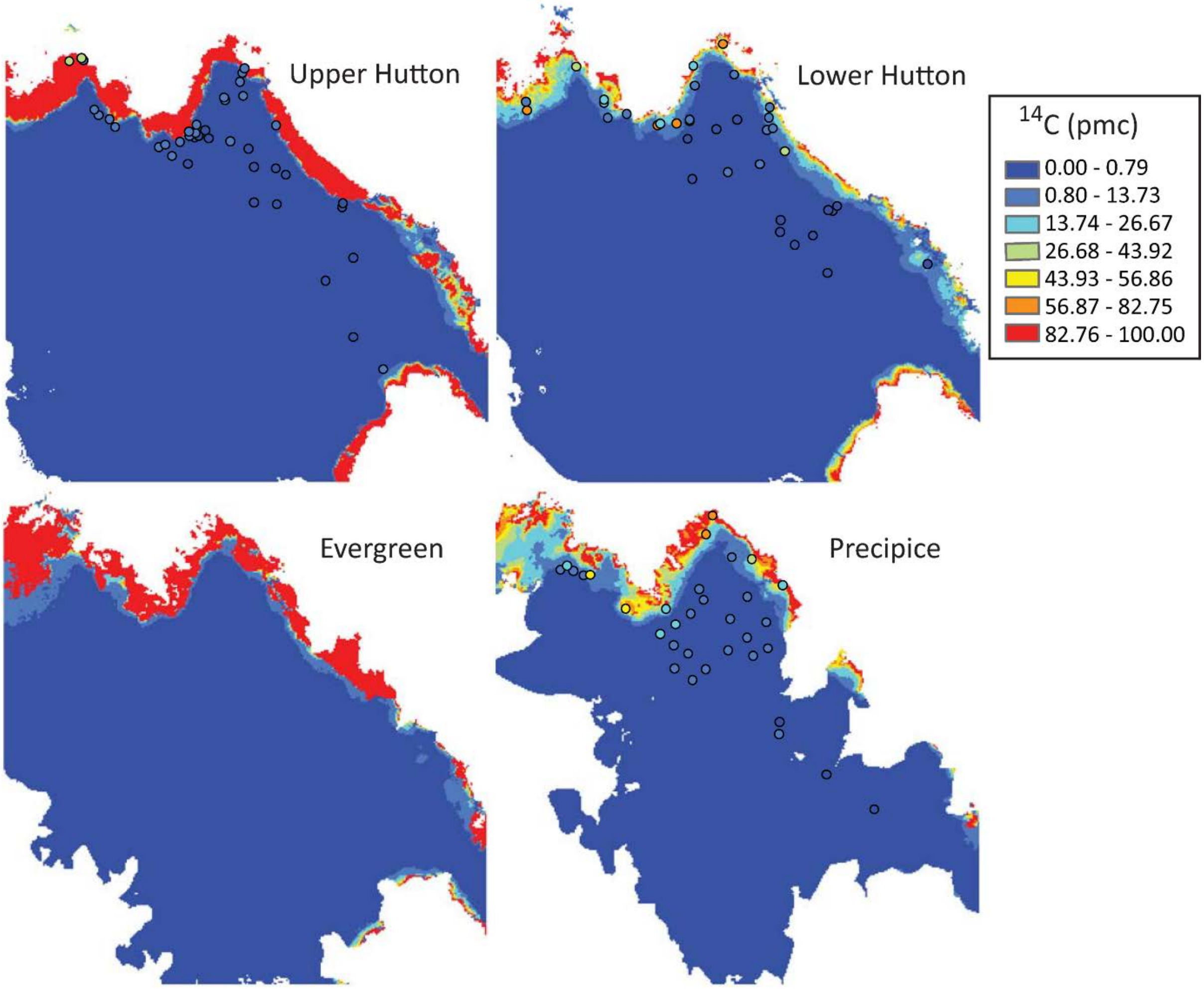

Figure 3.2: Initial simulation of (and observed) ^{14}C abundances for the Hutton down to the Precipice Sandstone aquifers using the single calibrated parameter set provided by OGIA (2016c).

3.2 Re-Calibration of the Hutton and Precipice Sandstone Aquifers Using Environmental Tracer Data

The parameters of the Hutton down to the Precipice Sandstone aquifers were refined, or re-calibrated, with the inclusion of ^{36}Cl and ^{14}C environmental tracer observations using the simulation procedure outlined in Section 2.3.3. The PEST++ software (*Welter et al.*, 2015), a parallel programming implementation of PEST using TCP/IP network communications, was used to conduct the calibration process in parallel on Pearcey, a high-performance compute cluster operated by CSIRO. Since there were 64 parameters, only a maximum of 65 cores were required to conduct this analysis assuming forward difference approximation of derivatives (i.e., for estimating a Jacobian matrix). Figures 16 and 17 illustrate the re-calibrated tracer distributions focussed on the northern regions for ^{36}Cl, where most of these data were sampled. Figures 18 and 19 display the observed versus simulated ^{36}Cl and hydraulic head results on 1-to-1 plots. The estimated spatially distributed parameters are depicted in Figures 20-22. The estimated horizontal and vertical hydraulic conductivity for the Evergreen Formation was 5.24×10^{-5}m/d and 1.00×10^{-7} m/d, respectively. The estimated recharge multipliers compared to those estimated by *OGIA* (2016c) are listed in Table 3.1. A detailed list of each individual parameter and its associated statistics are provided in Appendix A.

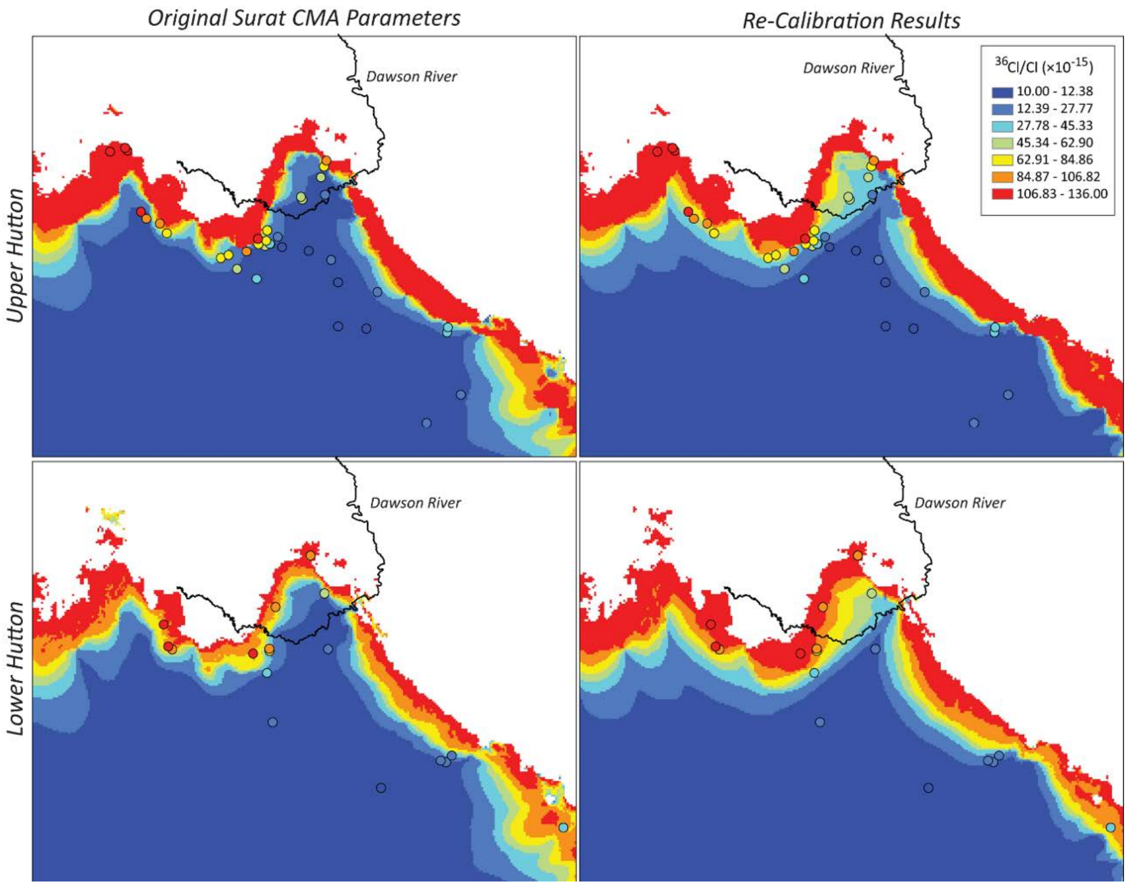

Figure 3.3. Simulated and observed ^{36}Cl abundances for the Hutton Sandstone. The results associated with the original single parameter set provided by OGIA (2016c) are compared with the re-calibrated results obtained in this study.

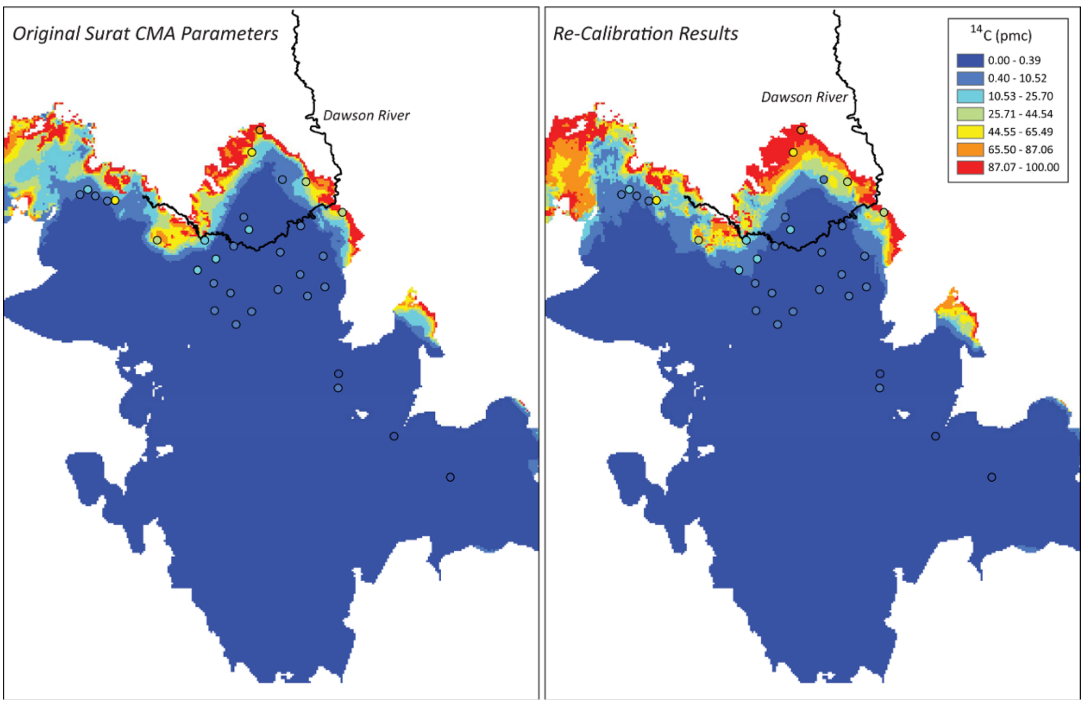

Figure 3.4. Simulated and observed ^{14}C abundances for the Precipice Sandstone. The results associated with the original single parameter set provided by OGIA (2016c) are compared with the re-calibrated results obtained in this study.

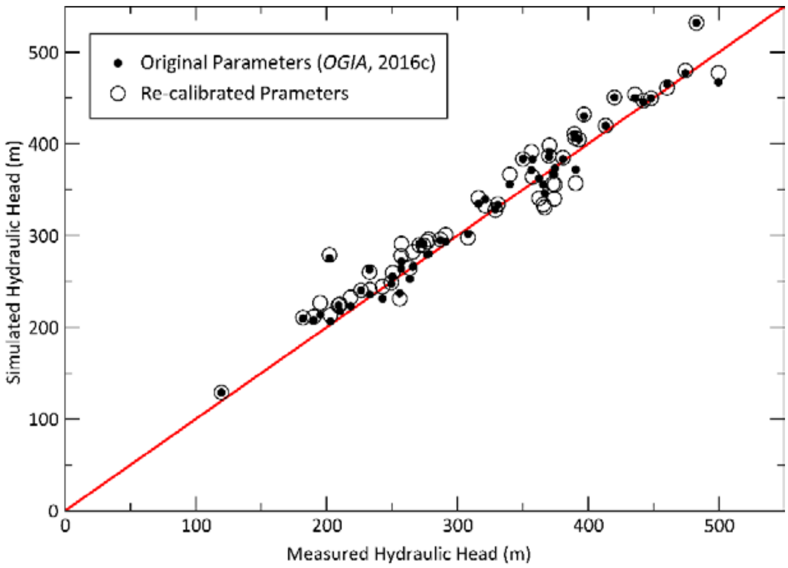

Figure 3.5. Comparison of measured hydraulic head with its simulated equivalent on 1-to-1 plot. The results associated with the original single parameter set provided by OGIA (2016c) are compared with the re-calibrated results obtained in this study.

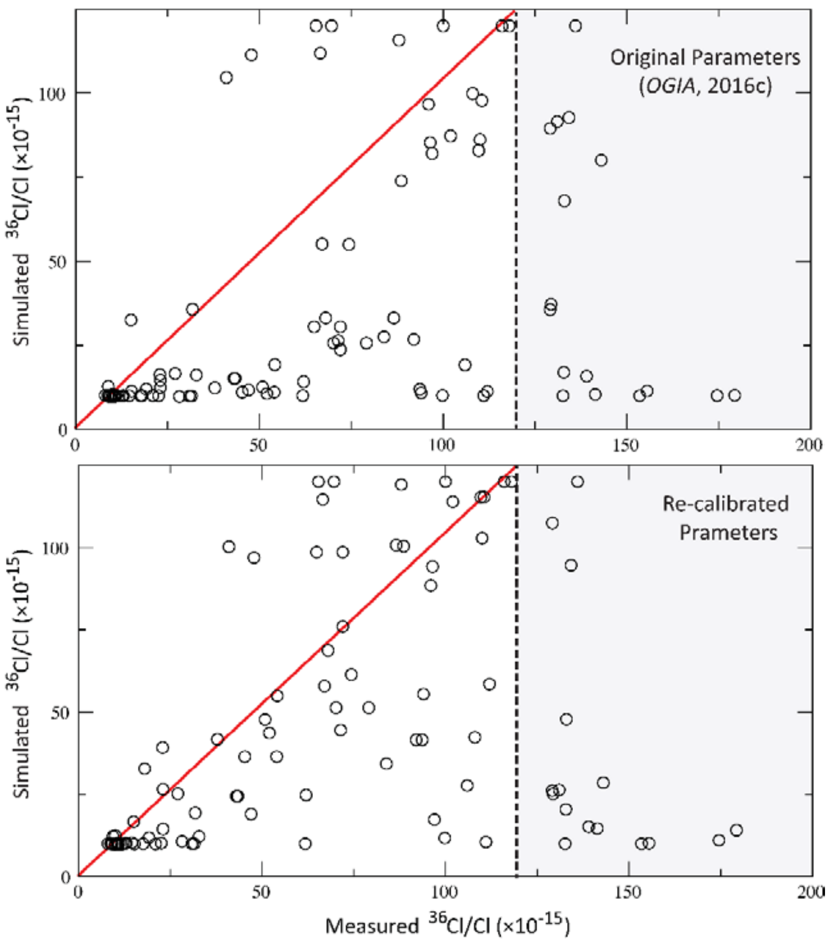

Figure 3.6. Comparison of measured ^{36}Cl abundance with its simulated equivalent on 1-to-1 plot. The results associated with the original single parameter set provided by *OGIA* (2016c) are compared with the re-calibrated results obtained in this study. The grey region indicates values that are not possible to match due to the incoming recharge being assigned a uniform abundance of 120×10^{-15}.

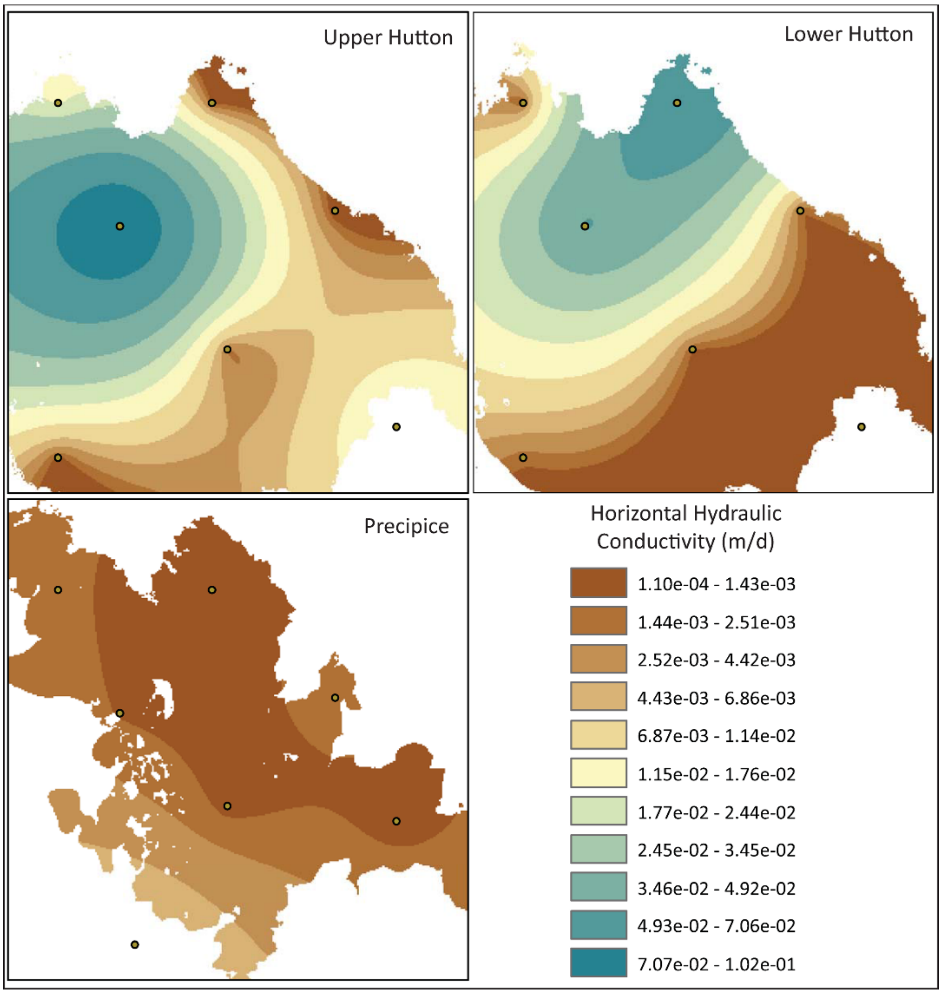

Figure 3.7. Estimated horizontal hydraulic conductivity.

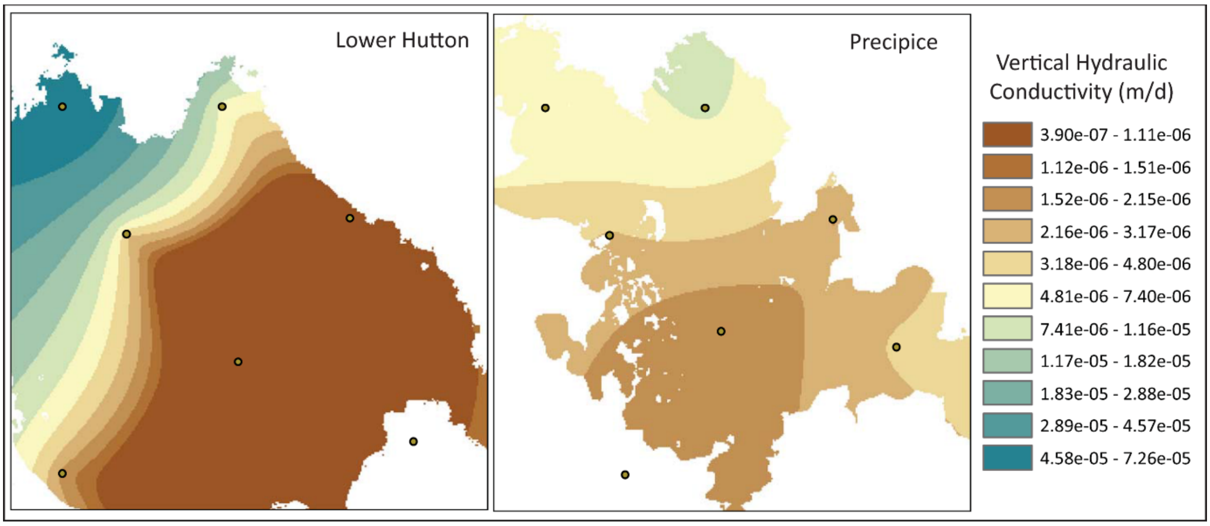

Figure 3.8. Estimated vertical hydraulic conductivity.

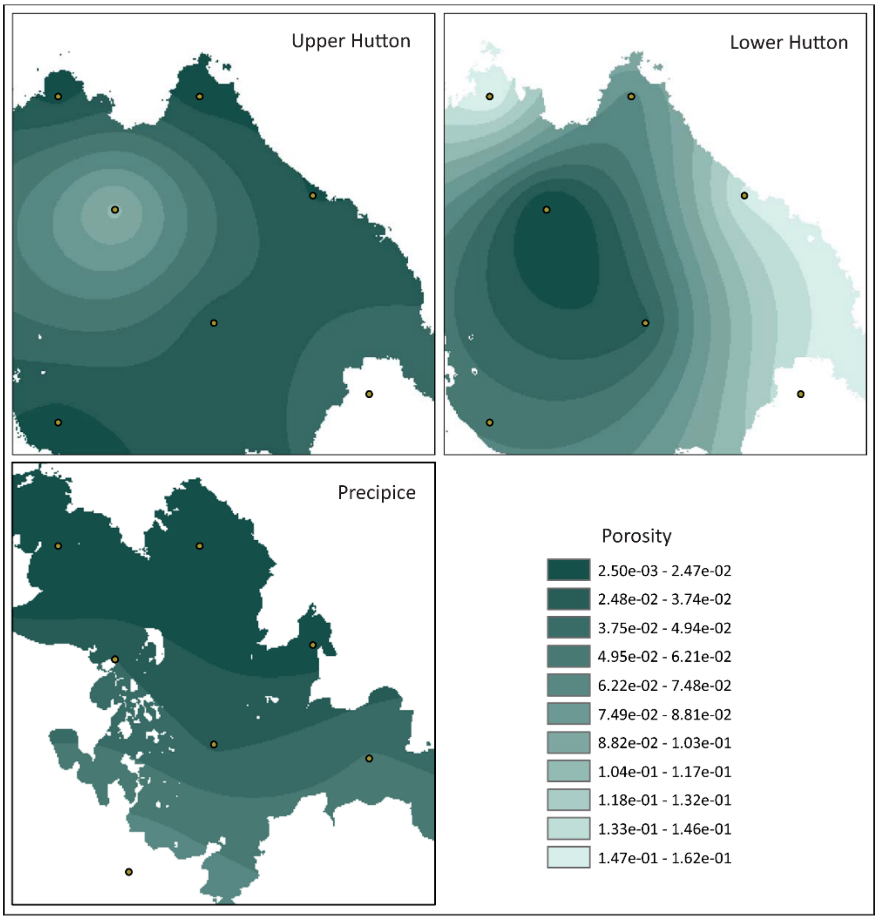

Figure 3.9. Estimated porosity.

The calibration process continues to reproduce the hydraulic head measurements as well as the original parameter set provided by *OGIA* (2016c). In many areas, the re-calibration results produce a slightly worse result, but in some areas the residuals are even reduced. Therefore, within the tolerance of measurement and model structural noise, the re-calibration hydraulic head results are adequate. However, without additional constraints such as environmental tracer data, these data could be easily matched for a number of different combinations of parameters.

The environmental tracer distributions for ^{36}Cl are significantly improved upon re-calibration of the properties in the Hutton Sandstone down to the Precipice Sandstone. Overall, the original parameter set provided by *OGIA* (2016c) underestimates the ^{36}Cl for the most part, with a few measurements being overestimated (Figure 3.6). The calibration procedure presented in this study dramatically shifted the data closer to the 1-to-1 line; however, there are still a number of observations that remain significantly underestimated. The most striking improvements in the calibration can be seen in the ^{36}Cl abundances of the Hutton Sandstone. Figure 3.5 shows a clear improvement for both model layers, with the calibration of the data in the Lower Hutton Sandstone in the very good agreement with the measured data. The estimated hydraulic properties produce an increased flow velocity off the outcrop areas, bringing younger groundwater further into the model domain. This is accomplished in part by the hydraulic conductivity in the northern regions being significantly greater than elsewhere in the aquifers. While this agrees somewhat with the parameter set provided by *OGIA* (2016c) in the Upper Hutton Sandstone (Figure 2.6), the results in the Lower Hutton Sandstone suggest that the hydraulic conductivity may be higher in this layer. However, the porosity estimates seem rather complimentary between the Upper Hutton and the Lower Hutton Sandstone, and are higher in magnitude in the Lower Hutton Sandstone, which reflects a complex correlation structure here. While beyond the scope of this study, additional sensitivity analyses could be conducted, using singular value decomposition techniques, to identify this correlation structure and to test whether or not it is possible to achieve a reasonable calibration with lower hydraulic conductivity and higher porosity estimates in the northern Lower Hutton Sandstone.

The calibration of the ^{14}C distributions in the Precipice Sandstone showed little improvement. This is due, in part, to the fact that many of the ^{14}C measurements indicate that the groundwater is quite old and are not providing much information for the calibration of regional hydraulic properties. This is reflected by the fact that the parameter estimates for the Precipice Sandstone remain relatively homogeneous (i.e., as suggested by their prior information constraints via Tikhonov regularisation) and do not stray much from their starting values. This insensitivity can also be seen in the composite scaled sensitivity and confidence interval results (Appendix A). Therefore, if larger starting values were assumed for horizontal hydraulic conductivity in the Precipice Sandstone, they may remain at these values during calibration and achieve the same overall level of model fit. Another potential reason for a lack of improvement in this calibration process could be due to potential conceptual model discrepancies, e.g., the outcrop coverage depicted in Figure 2.2 suggests that the Precipice Sandstone has a significant outcrop area in the north-western region; whereas, the model definition for this outcrop show little spatial coverage throughout the model domain. In fact, it appears that the Evergreen Formation's outcrop area in the model could be reassigned to the Precipice, as the vertical hydraulic conductivity of the Evergreen Formation should be relatively low. This could provide more potential for recharge in the Precipice Sandstone and a possibility to better match some of the higher ^{14}C abundances observed near the outcrops in the north-central region (Figure 3.4), thus increasing the sensitivity of the hydraulic properties in this formation to these data.

3.3 Recharge Estimates

The recharge multipliers estimated in this study agree very well with that estimated by *OGIA* (2016c); however, again, the estimated multiplier in the Precipice Sandstone remains quite uncertain due to the insensitivity of the parameters as mentioned previously (Table 3.1). The estimated recharge multiplier for the Hutton Sandstone aquifer appears to be very well constrained by the ^{36}Cl data. The estimated multiplier of the Evergreen Formation is the most uncertain with a relatively wide confidence interval as expected due to a lack of observation data and the fact that the very low vertical hydraulic conductivity of this formation likely results in significant rejected recharge.

Table 3.1. Pre and post-calibration recharge multipliers. Posterior estimated confidence intervals are based on a linearised approximation of the model using the log-transformation of parameters.

Aquifer	Estimated Recharge Multiplier		Estimated Confidence Interval	
	OGIA (2016c)	Re-Calibrated	Upper	Lower
Upper Hutton	**0.77**	**0.80**	**0.77**	**0.83**
Lower Hutton	**0.77**	**0.80**	**0.77**	**0.83**
Evergreen	**0.24**	**0.27**	**0.09**	**0.79**
Precipice	**0.12**	**0.10**	**0.04**	**0.28**

It should be mentioned here however, that these parameter estimates do not reflect an estimate of total net recharge into the aquifer systems for at least two reasons. First, due to the presence of drains in every model cell that receives recharge, there is a high potential for rejected recharge within each of these cells. This is a reasonable feature, as much of the precipitation is likely rejected due to the nature of the natural groundwater system. This leads to the second point in that the model can only discharge water primarily through the drains (discharge through the GHB's accounts for less than 1% of total natural discharge regardless of the uncertainty in parameter estimates). Therefore, from a regional perspective the discharge through drains is always equal to the recharge, e.g., the total net recharge in the Upper Hutton aquifer is about 0.0. Therefore, net recharge is a local phenomenon and spatially distributed along the outcrop areas, with a high degree of simulated variability based in drain elevation and hydraulic head.

3.4 Mean Age Simulations

Upon calibration of environmental tracer data (i.e., calibrating the model to tracer abundance itself without interpreting a groundwater "age" beforehand), the three-dimensional numerical model for reactive transport developed in this study can be used to simulate mean age. The term "mean age" is used to indicate that the simulated age of groundwater at a point in the domain represents a mixture of groundwater with different ages explicitly simulated by the model. This is accomplished by defining incoming recharge water at the outcrops to have a "concentration" of zero and subjecting this water to a 0th-order production rate that is equivalent with time itself. That is, if the state variable is to represent years of age and the time unit of the model was years, the production rate would be simply $1.00\ \mathrm{mg/L\ yr^{-1}}$, and if the time unit were days it would be $2.38 \times 10^{-3}\ \mathrm{mg/L\ yr^{-1}}$. This was also applied to the connection of the alluvium and basalt aquifers with the Upper Hutton Sandstone (as was done with the environmental tracers). The simulation was run for both the original parameters provided by *OGIA* (2016c) and the re-calibrated parameters in steady-state (Figure 3.10).

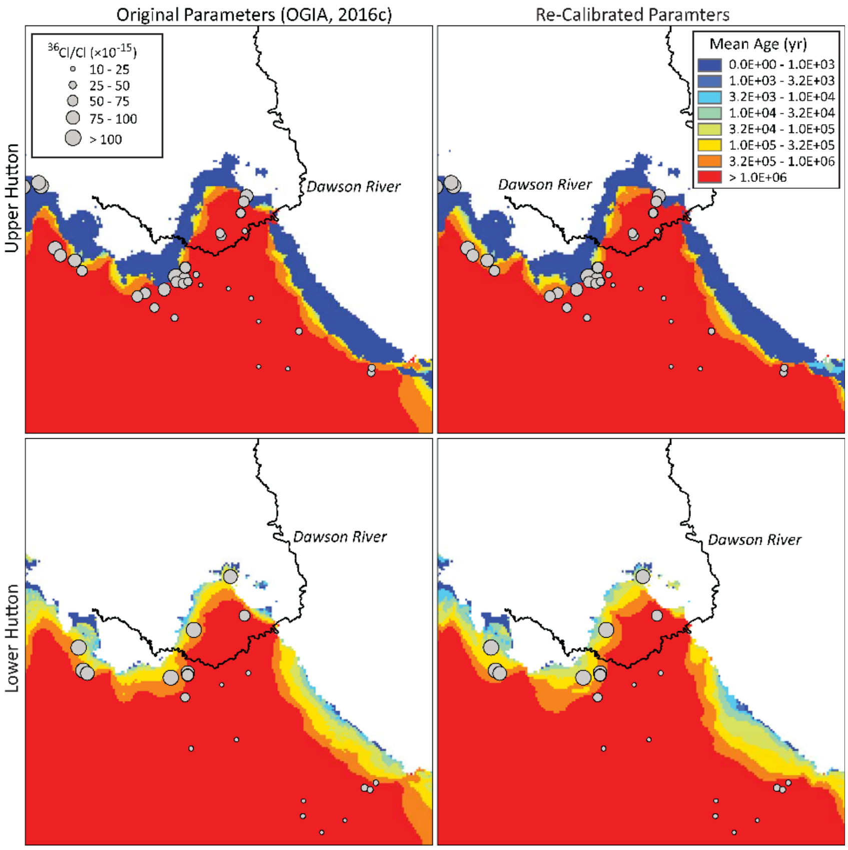

Figure 3.10. Simulated mean age distributions along with measured ^{36}Cl abundances. The results of the original parameter set provided by OGIA (2016c) and the re-calibrated parameter set are compared.

The mean age simulation results indicate that even in the relative close vicinity to the outcrop areas the groundwater is well over a million years old. This is contradictory to the current interpretation of the environmental tracers which would indicate that the groundwater is instead on the order of 10's or 100's of thousands of years old in this region. This interpretation of the tracer data alone clearly demonstrates the inability to accurately use simplified models to describe groundwater age, as in Equation 1 or other one-dimensional analytical models. The discrepancy likely lies mainly with mixing of old and young groundwater and the subsurface production of ^{36}Cl. For example, the ^{36}Cl measurement in the Lower Hutton Sandstone nearest to the outcrop areas around the Dawson River is well-calibrated by the model (Figure 3.3). If the measured or the simulated ^{36}Cl/Cl value was used with Equation 1, the estimated age of the groundwater would be on the order of about 400,000 years old; however, the mean age simulation indicates that the groundwater is instead about five million years old in this region (Figure 3.10). This is a dramatic difference that clearly demonstrates the benefit associated with the explicit inclusion of mixing and production via three-dimensional numerical modelling on the interpretation of ^{36}Cl groundwater age.

This discrepancy in groundwater ages is even more dramatic when using the original parameters provided by *OGIA* (2016c). However, upon re-calibration of the ^{36}Cl data, the younger water travels further into the model domain in the Lower Hutton Sandstone, as indicated by the mean age simulations (Figure 3.10). However, it is also important to note that the differences in the mean age simulation between the two parameters is less pronounced in the Upper Hutton Sandstone and yet, the simulated ^{36}Cl distributions are dramatically different in this model layer (Figure 3.3). This indicates that effects of mixing and ^{36}Cl production are less pronounced in the Upper Hutton Sandstone, which is intuitive since there is likely to be less mixing of older groundwater in this layer than in the Lower Hutton Sandstone. The mean age simulations of the Precipice Sandstone indicate that groundwater is much older than expected, which is likely a result of a poor model fit to ^{14}C data, resulting from potential model conceptualisation considerations. This is however a good result in that it demonstrates how the numerical simulation of environmental tracers can guide the development of conceptual models.

4 Conclusions and Future Directions

The analysis conducted in this study demonstrates that the information content associated with environmental tracer observations can be significant within a numerical modelling context. We have included ^{36}Cl and ^{14}C tracer data within a robust modelling and calibration framework to enhance the estimation of hydraulic properties. This modelling framework exploits the substantial amount of hydrogeological knowledge of the Surat CMA by utilising the associated regional numerical model developed by OGIA (2106c) to derive groundwater flow fields. The study developed and tested an effective workflow that can be used to extract flow fields from the OGIA model for subsequent use within a subdomain surrogate model. This procedure allowed for the employment of the widely used solute transport code MT3DMS for the simulation of the reactive transport of multiple environmental tracers. For the simulation of ^{36}Cl the MT3DMS source code required modification to allow for the simultaneous simulation of decay and production of ^{36}Cl. With the modified code it was feasible to provide the first data-constrained modelling study to consider the regional-scale three-dimensional simulation of 36Cl under consideration of both decay and production of ^{36}Cl.

The calibrated model reproduced the ^{36}Cl data well and provided a range of new insights into potential modifications for the (re-)parameterisation of the Surat CMA model. The results indicate, for example, that the hydraulic conductivity in the Lower Hutton Sandstone is likely greater than current estimates. However, the hydraulic properties of the Precipice Sandstone still remain uncertain due to the insensitivity of the ^{14}C data and perhaps due to conceptual model considerations. This is likely due to the relatively old age of much of the groundwater in the aquifers of interest, which may be beyond the age limit of ^{14}C in the interior of the basin. However, while beyond the scope of the present study, the development of one or more two-dimensional, cross-sectional reactive transport models extending from the Hutton and Precipice Sandstone outcrops into the interior of the basin, along selected flow paths (which can be deduced from this study), could be constructed to make effective use of the ^{14}C data near outcrops and better estimate localised net recharge rates.

Using the calibrated reactive transport model, mean age simulations demonstrate the significant impact of mixing and ^{36}Cl production on the interpretation of groundwater age using simplified models. For example, the simulated mean age in the Lower Hutton Sandstone near the Dawson River is about ten times larger than the groundwater age interpreted from Equation 1 with ^{36}Cl.

Overall, the results show that both the potentiometric surface and the observed environmental tracer data can be simultaneously reproduced by the three-dimensional numerical model. The insights gained form this numerical modelling study also highlights that the flow system is far too complex to be interpreted by simplistic one-dimensional approaches. Recharge in the Surat Basin is likely being discharged to the eastern outcrop areas near the Dawson River, but future research is required to better quantify localised net recharge rates and the possibility that recharge in the Surat Basin also contributes recharge to the Great Artesian Basin.

While beyond the scope of the present study, the direct simulation of helium as an additional environmental tracer has significant potential for acquiring information for both younger waters and the very old groundwater in deeper aquifer systems beyond the temporal reach of ^{36}Cl and ^{14}C data. This is because changes in the accumulation and transport of helium is likely to be sensitive to the entire flow field regardless of age, i.e., the distribution of helium in very old groundwater (more than one million years) may be highly variable, where for example, ^{36}Cl would be relatively uniform (at its average secular equilibrium) and ^{14}C would be negligible (at about 0 pmc).

Environmental tracers can provide a great deal of useful information; however, measuring environmental tracers in the field is expensive and often requires significant expertise to be handled properly. As a result, the location and type of measurement to be taken must be chosen very carefully, which may not be straightforward. However, with emerging data worth and experimental design techniques, numerical models can increasingly be used to determine where and what data type should be collected to maximise information about a particular objective. For example, one could develop a sampling design aimed at estimating net recharge at a specific location, or one may be interested in using environmental tracers to better estimate hydraulic properties sensitive to the future predictions of CSG operations. Combinatorial issues that arise when considering many samples at once can be handled with heuristic optimisation techniques (*Wöhling et al.*, 2016) and parameter uncertainty effects can be handled with robust maximin optimisation methods (*Siade et al.*, 2017). Furthermore, the information associated with one tracer may magnify the information associated with another (e.g., ^{4}He informing on ^{14}C, or ^{81}Kr informing on ^{36}Cl, etc.). These effects can also be considered in developing a sampling design and remain a topic of future research.

References

APLNG, (2014), *Australia Pacific LNG Upstream 2013-2014 Groundwater Assessment Report*. Available at http://www.aplng.com.au/pdf/Q-LNG01-75-RP-0001__Annual_GW__Report_Rev1_Final.pdf.

Bentley, H., Phillips, F.M., Davis, S.N., Habermehl, M.A., Airey, P.L., Calf, G.E., Elmore, D., Gove, H.E., Torgersen, T., (1986), Chlorine-36 dating of very old groundwater: The Great Artesian Basin, Australia, *Water Resources Research*, 22, 1991-2001. https://doi.org/10.1029/WR022i013p01991.

Castro, M.C., Goblet, P., (2003), Calibration of regional groundwater flow models: Working toward a better understanding of site-specific systems, *Water Resources Research*, 39(6), 1172, https://doi.org/10.1029/2002WR001653.

Cook, P.G., Herczeg, A.L., (2000), *Environmental Tracers in Subsurface Hydrology*. Kluwer, Boston, 529p.

Cook, P.G., Robinson, N.I., (2002), Estimating groundwater recharge in fractured rock from environmental ^{3}H and ^{36}Cl, Clare Valley, South Australia, *Water Resources Research*, 38(8), https://doi.org/10.1029/2001wr000772.

Cussler, E.L., (2009), *Diffusion: Mass Transfer in Fluid Systems*, Cambridge University Press, Cambridge.

Doherty, J.E. (2016a). *Model-independent parameter estimation user manual Part I: PEST, SENSAN and global optimisers*. Brisbane, Australia: Watermark Numerical Computing.

Doherty, J.E. (2016b). *Model-independent parameter estimation user manual Part II: PEST utility support software*. Brisbane, Australia: Watermark Numerical Computing.

Feitz, A., Ransley, T., Hodgkinson, J., Preda, M., Dunsmore, R., McKillop, J., Spulak, R., Dixon, O., Kuske, T., and Draper, J., (2014), *GA-GSQ Hydrochemistry dataset (2009-2011)*. GEOCAT No. 78549, Geoscience Australia, Canberra.

GHD, 2012, *Report for Queensland Water Commission (QWC), Stage 2 Surat Cumulative Management Area Groundwater Model Report*, Office of Groundwater Impact Assessment, Brisbane.

Guiton, S., Kieft, R., Churchill, J., Sheerin, C., (2015), Characterising the Hutton Sandstone in the Northeastern Surat Basin. In '*AAPG Asia Pacific Region, Geoscience Technology Workshop, Opportunities in Coal Bed Methane in the Asia Pacific. Brisbane*'. (Ed. AAP Region). Available at http://www.searchanddiscovery.com/abstracts/pdf/2015/90234gtw/abstracts/ndx_guiton.pdf.

Habermehl, M.A., Devonshire, J., Magee, J.W., (2009), *Sustainable groundwater allocations in the intake beds of the Great Artesian Basin in New South Wales: Final report*, Bureau of Rural Sciences, Canberra.

Hodgkinson, J., Hortle, A., McKillop, M., (2010), The Application of Hydrodynamic Analysis in the Assessment of Regional Aquifers for Carbon Geostorage: Preliminary Results for the Surat Basin, Queensland. *APPEA Journal, 50*(1), 445-462. https://doi.org/10.1071/AJ09027.

IAEA, (2013), *Isotope Methods for Dating Old Groundwater*. International Atomic Energy Agency, Vienna.

Kellett, J.R., Ransley, T.R., Coram, J., Jaycock, J., Barclay, D.F., McMahon, G.A., Foster, L.M., Hillier, J.R., (2003), *Groundwater recharge in the Great Artesian Basin Intake beds, Queensland*. Final Report for NHT Project 982713 Sustainable Groundwater use in the GAB Intake Beds, Natural Resources and Mines, Queensland.

Konikow, L.F., Bredehoeft, J.D., (1992), Groundwater models cannot be validated, *Advances in Water Resources*, 15(1), 71-83, https://doi.org/10.1016/0309-1708(92)90033-X.

Leray, S., de Dreuzy, J.-R., Bour, O., Labasque, T., Aquilina, L., (2012), Contribution of age data to the characterization of complex aquifers, *Journal of Hydrology*, (464–465), 54-68. https://doi.org/10.1016/j.jhydrol.2012.06.052.

Lehmann, B.E., Love, A., Purtschert, R., Collon, P., Loosli, H.H., Kutschera, W., Beyerle, U., Aeschbach-Hertig, W., Kipfer, R., Frape, S.K., Herczeg, A., Moran, J., Tolstikhin, I.N., Gröning, M., (2003), A comparison of groundwater dating with ^{81}Kr, ^{36}Cl and ^{4}He in four wells of the Great Artesian Basin, Australia, *Earth and Planetary Science Letters*, 211(3–4), 237-250, https://doi.org/10.1016/S0012-821X(03)00206-1.

Love, A.J., Herczeg, A.L., Sampson, L., Cresswell, R.G., Fifield, L.K., (2000), Sources of chloride and implications for ^{36}Cl dating of old groundwater, southwestern Great Artesian Basin, Australia, *Water Resources Research*, 36(6), 1561-1574, https://doi.org/10.1029/2000WR900019.

Mahara, Y., Habermehl, M.A., Hasegawa, T., Nakata, K., Ransley, T.R., Hatano, T., Mizuochi, Y., Kobayashi, H., Ninomiya, A., Senior, B.R., Yasuda, H., Ohta, T., (2009), Groundwater dating by estimation of groundwater flow velocity and dissolved ^{4}He accumulation rate calibrated by ^{36}Cl in the Great Artesian Basin, Australia, *Earth and Planetary Science Letters,* (287), 43-56. https://doi.org/10.1016/j.epsl.2009.07.034.

Michael, H.A., Voss, C.I., (2009), Controls on groundwater flow in the Bengal Basin of India and Bangladesh: regional modeling analysis, *Hydrogeology Journal*, 17(7), 1561-1577. https://doi.org/10.1007/s10040-008-0429-4.

OGIA, (2016a), *Hydrogeological conceptualisation report for the Surat Cumulative Management Area*. Department of Natural Resources and Mines, Office of Groundwater Impact Assessment, Brisbane.

OGIA, (2016b), *Underground Water Impact Report for the Surat Cumulative Management Area*, Department of Natural Resources and Mines, Office of Groundwater Impact Assessment, Brisbane.

OGIA, (2016c), *Groundwater modelling report for the Surat Cumulative Management Area*, Department of Natural Resources and Mines, Office of Groundwater Impact Assessment, Brisbane.

Panday, S., Langevin, C.D., Niswonger, R.G., Ibaraki, M., and Hughes, J.D., (2017), *MODFLOW-USG version 1.4.00: An unstructured grid version of MODFLOW for simulating groundwater flow and tightly coupled processes using a control volume finite-difference formulation*: U.S. Geological Survey Software Release, https://dx.doi.org/10.5066/F7R20ZFJ.

Park, J., Bethke, C.M., Torgersen, T., Johnson, T., (2002), Transport modeling applied to the interpretation of groundwater ^{36}Cl age, *Water Resources Research*, 38(5), https://doi.org/10.1029/2001WR000399.

Patterson L.J., Sturchio N.C., Kennedy B.M., van Soest M.C., Sultan M., Lu, Z.-T., Lehmann, B., Purtschert, R., El Alfy, Z., El Kaliouby, B., Dawood, Y., Abdallah, A., (2005), Cosmogenic, radiogenic, and stable isotopic constraints on groundwater residence time in the Nubian Aquifer, Western Desert of Egypt, *Geochemistry Geophysics Geosystems*, (6), Q01005, https://doi.org/10.1029/2004GC000779.

Radke, B.M., Ferguson, J., Cresswell, R.G., Ransley, T.R., Habermehl, M.A., (2000), *Hydrochemistry and implied hydrodynamics of the Cadna-Owi–Hooray Aquifer, Great Artesian Basin*, *Australia*, Bureau of Rural Sciences, Canberra.

Raiber, M., Suckow, A., (2017), *Hydrochemical assessment of the Hutton and Precipice sandstones in the northern Surat Basin*. CSIRO, Australia, CSIRO, Australia. Available at https://gisera.org.au/wp-content/uploads/2015/11/Water-6-Report-Milestone-3.1-JUNE-2017.pdf.

Ransley, T.R., Smerdon, B.D., (2012). *Hydrostratigraphy, hydrogeology and system conceptualisation of the Great Artesian Basin*. CSIRO Water for a Healthy Country Flagship, Australia.

Ransley, T.R., Somerville, P.D., Tan, K.P., Feitz, A.J., Cook, S., Yates, G., Schoning, G., Caruana, L., Sundaram, B., Wallace, L.J., (2015), *Groundwater hydrochemical characterisation of the Surat Region and Laura Basin - Queensland*. Record 2015/05. Geoscience Australia, Canberra. https://doi.org/10.11636/Record.2015.005.

Reilly, T.E., Plummer, L.N., Phillips, P.J., Busenberg, E., (1994), The Use of Simulation and Multiple Environmental Tracers to Quantify Groundwater-Flow in a Shallow Aquifer, *Water Resources Research*, 30(2), 421-433. https://doi.org/10.1029/93wr02655.

Salmon, S.U., Prommer, H., Park, J., Meredith, K.T., Turner, J.V., MaCallum, J.L., (2015), A general reactive transport modeling framework for simulating and interpreting groundwater ^{14}C age and δ^{13}C, *Water Resources Research*, 51, 359–376, https://doi.org/10.1002/2014WR015779.

Sanford, W.E., Plummer, L.N., McAda, D.P., Bexfield, L.M., Anderholm, S.K., (2004), Hydrochemical tracers in the middle Rio Grande Basin, USA: 2. Calibration of a groundwater-flow model, *Hydrogeology Journal*, 12(4), 389-407. https://doi.org/10.1007/s10040-004-0326-4.

Sanford, W.E., (2011), Calibration of models using groundwater age, *Hydrogeology Journal*, 19(1), 13-16. https://doi.org/10.1007/s10040-010-0637-6.

Siade, A. J., Hall, J., and Karelse, R. N., (2017)., A practical, robust methodology for acquiring new observation data using computationally expensive groundwater models, *Water Resources Research*, (53). https://doi.org/10.1002/2017WR020814.

Smith, S.D., (2015), *Geochemical baseline monitoring: quartz-helium trial*. CSIRO, Adelaide. Available at https://gisera.org.au/wp-content/uploads/2012/06/BaselineChem_Quartz-He_report-March-2015.pdf.

Solomon, D.K., Schiff, S.L., Poreda, R.J., Clarke, W.B., (1993), A validation of the ^{3}H/^{3}He method for determining groundwater recharge, *Water Resources Research*, 29(9), 2951-2962. https://doi.org/10.1029/93WR00968.

Sreekanth, J., Moore, C., (2015), *CSG Water Reinjection Impacts: Modelling, Uncertainty and Risk Analysis; Groundwater flow and transport modelling and uncertainty analysis to quantify the water quantity and quality impacts of a coal seam gas produced water reinjection scheme in the Surat Basin, Queensland*. CSIRO Land and Water Flagship.

Suckow, A., (2014), The age of groundwater – Definitions, models and why we do not need this term, *Applied Geochemistry* 50, 222-230. https://doi.org/10.1016/j.apgeochem.2014.04.016.

Suckow, A., Taylor, A.R., Davies, P., Leaney, F.W., (2016), *Geochemical Baseline Monitoring. Final Report*: CSIRO, Australia. Available at https://gisera.csiro.au/wp-content/uploads/2018/03/Water-4-Final-Report-2016.pdf

Suckow, A., Raiber, M., Deslandes, A., Gerber, C., (2018), *Constraining conceptual groundwater models for the Hutton and Precipice aquifers in the Surat Basin through tracer data*: CSIRO, Australia, *in press*.

Torgersen, T., Habermehl, M.A., Phillips, F.M., Elmore, D., Kubik, P., Geoffrey-Jones, B., Hemmick, T., Gove, H.E., (1991), Chlorine-36 dating of very old groundwater. Further studies in the Great Artesian Basin, Australia, *Water Resources Research*, 27, 3201-3213. https://doi.org/10.1029/91WR02078.

Turnadge, C., Smerdon, B.D., (2014), A review of methods for modelling environmental tracers in groundwater: Advantages of tracer concentration simulation, *Journal of Hydrology*, 519, 3674-3689. https://doi.org/10.1016/j.jhydrol.2014.10.056.

Vogel, J.C., Thilo, L., Vandijken, M., (1974), Determination of Groundwater Recharge with Tritium, *Journal of Hydrology*, 23(1-2), 131-140. https://doi.org/10.1016/0022-1694(74)90027-4

Weiss, R., Smith, L., (1998), Parameter space methods in joint parameter estimation for groundwater flow models, *Water Resources Research*, 34(4), 647–661, https://doi.org/10.1029/97WR03467.

Welter, D. E., White, J. T., Hunt, R. J., & Doherty, J. E. (2015). *Approaches in highly parameterized inversion—PEST++ Version 3, a Parameter ESTimation and uncertainty analysis software suite optimized for large environmental models*. In U.S. Geological Survey Techniques and Methods (Book 7, Chapter C12). Reston, VA: U.S. Geological Survey.

Wöhling, T., Geiges, A., and Nowak, W., (2016), Optimal design of multitype groundwater monitoring networks using easily accessible tools, *Groundwater*, (54), 861–870. https://doi.org/10.1111/gwat.12430.

Yager, R.M., Plummer, L.N., Kauffman, L.J., Doctor, D.H., Nelms, D.L., Schlosser, P., (2013), Comparison of age distributions estimated from environmental tracers by using binary-dilution and numerical models of fractured and folded karst: Shenandoah Valley of Virginia and West Virginia, USA, *Hydrogeology Journal*, 21(6), 1193-1217. https://doi.org/10.1007/s10040-013-0997-9.

Zheng, C. & Wang, P.P., (1999), *MT3DMS: A Modular Three-Dimensional Multispecies Transport Model for Simulation of Advection, Dispersion, and Chemical Reactions of Contaminants in Groundwater Systems; Documentation and User's Guide.* Prepared for the U.S. Army Corps of Engineers.

Zimmerman, D. A., de Marsily, G., Gotway, C. A., Marietta, M. G., Axness, C. L., Beauhelm, R. L., Bras, R. L., Carrera, J., Dagan, G., Davies, P. B., Gallegos, D. P., Galli, A., Gomez-Hernandez, J., Grindrod, P., Gutjahr, A. L., Kitanidis, P. K., Lavenue, A.M., McLaughlin, D., Neuman, S. P., RamaRao, B. S., Ravenne, C., Rubin Y., (1998), A comparison of seven geostatistically based inverse approaches to estimate transmissivities for modeling advective transport by groundwater flow, *Water Resources Research*, 34(6), 1373-1413. https://doi.org/10.1029/98WR00003.

Appendix A

Apx Table A.1 Estimated horizontal hydraulic and relevant calibration statistics. All calculations are based on the log-transformation of the parameters. The parameter names indicate the layer and the pilot point number in Figure 2.12, i.e., "PPHK02-01" is layer 2 (Upper Hutton), pilot point #1. Confidence limits are based on 95% confidence, i.e., +/- two standard deviations.

Name	Initial Value	Prior Confidence Limits Lower	Prior Confidence Limits Upper	Estimated Value	Posterior Confidence Limits Lower	Posterior Confidence Limits Upper	Composite Scaled Sensitivity
PPHK02-01	1.00E-03	3.16E-06	3.16E-01	1.68E-02	1.51E-02	1.87E-02	1.85E-04
PPHK02-02	1.00E-03	3.16E-06	3.16E-01	1.12E-03	7.72E-04	1.63E-03	8.16E-05
PPHK02-03	1.00E-03	3.16E-06	3.16E-01	2.61E-04	4.67E-06	1.46E-02	1.62E-04
PPHK02-04	1.00E-03	3.16E-06	3.16E-01	1.89E-02	1.65E-02	2.17E-02	2.57E-03
PPHK02-05	1.00E-03	3.16E-06	3.16E-01	9.30E-04	1.24E-05	6.99E-02	3.34E-05
PPHK02-06	1.00E-03	3.16E-06	3.16E-01	1.02E-01	9.83E-02	1.07E-01	3.30E-04
PPHK02-07	1.00E-03	3.16E-06	3.16E-01	2.36E-03	1.38E-04	4.03E-02	1.26E-05
PPHK03-01	1.00E-03	3.16E-06	3.16E-01	1.75E-03	6.06E-04	5.04E-03	2.31E-05
PPHK03-02	1.00E-03	3.16E-06	3.16E-01	7.19E-02	6.81E-02	7.59E-02	5.01E-04
PPHK03-03	1.00E-03	3.16E-06	3.16E-01	1.60E-04	1.18E-05	2.16E-03	1.12E-04
PPHK03-04	1.00E-03	3.16E-06	3.16E-01	7.92E-04	4.68E-06	1.34E-01	6.07E-06
PPHK03-05	1.00E-03	3.16E-06	3.16E-01	1.83E-03	1.83E-03	1.83E-03	4.10E-01
PPHK03-06	1.00E-03	3.16E-06	3.16E-01	5.02E-02	4.48E-02	5.62E-02	1.54E-04
PPHK03-07	1.00E-03	3.16E-06	3.16E-01	1.33E-03	1.15E-05	1.54E-01	1.33E-05
PPHK04-01	1.00E-04	3.16E-07	3.16E-02	5.24E-05	4.08E-05	6.74E-05	1.26E-04
PPHK05-01	1.00E-03	3.16E-06	3.16E-01	1.63E-04	3.29E-05	8.10E-04	7.87E-05
PPHK05-02	1.00E-03	3.16E-06	3.16E-01	1.11E-04	1.84E-05	6.71E-04	1.94E-04
PPHK05-03	1.00E-03	3.16E-06	3.16E-01	1.93E-03	1.51E-03	2.46E-03	2.75E-04
PPHK05-04	1.00E-03	3.16E-06	3.16E-01	1.10E-03	3.02E-05	4.03E-02	2.90E-05
PPHK05-05	1.00E-03	3.16E-06	3.16E-01	7.60E-03	2.11E-03	2.74E-02	6.18E-05
PPHK05-06	1.00E-03	3.16E-06	3.16E-01	1.35E-03	1.23E-03	1.47E-03	2.43E-03
PPHK05-07	1.00E-03	3.16E-06	3.16E-01	1.08E-03	3.07E-05	3.81E-02	5.98E-05

Apx Table A.2 Estimated vertical hydraulic and relevant calibration statistics. All calculations are based on the log-transformation of the parameters. The parameter names indicate the layer and the pilot point number in Figure 2.12, i.e., "PPVK02-01" is layer 2 (Upper Hutton), pilot point #1. Confidence limits are based on 95% confidence, i.e., +/- two standard deviations.

Name	Initial Value	Prior Confidence Limits Lower	Prior Confidence Limits Upper	Estimated Value	Posterior Confidence Limits Lower	Posterior Confidence Limits Upper	Composite Scaled Sensitivity
PPVK03-01	1.00E-06	1.00E-09	1.00E-03	7.27E-05	6.14E-05	8.62E-05	3.02E-04
PPVK03-02	1.00E-06	1.00E-09	1.00E-03	6.17E-06	5.25E-06	7.26E-06	5.12E-04
PPVK03-03	1.00E-06	1.00E-09	1.00E-03	3.90E-07	1.18E-07	1.29E-06	3.58E-04
PPVK03-04	1.00E-06	1.00E-09	1.00E-03	6.38E-07	4.90E-07	8.29E-07	8.56E-03
PPVK03-05	1.00E-06	1.00E-09	1.00E-03	1.81E-06	2.06E-09	1.59E-03	6.28E-06
PPVK03-06	1.00E-06	1.00E-09	1.00E-03	3.42E-06	2.20E-07	5.32E-05	3.57E-05
PPVK03-07	1.00E-06	1.00E-09	1.00E-03	8.35E-07	7.43E-08	9.38E-06	9.74E-04
PPVK04-01	1.00E-07	1.00E-10	1.00E-04	1.00E-07	1.00E-10	1.00E-04	0.00E+00
PPVK05-01	1.00E-06	1.00E-09	1.00E-03	6.46E-06	4.38E-08	9.52E-04	1.63E-05
PPVK05-02	1.00E-06	1.00E-09	1.00E-03	7.89E-06	5.74E-07	1.08E-04	2.69E-05
PPVK05-03	1.00E-06	1.00E-09	1.00E-03	2.13E-06	5.34E-07	8.47E-06	3.65E-04
PPVK05-04	1.00E-06	1.00E-09	1.00E-03	3.33E-06	3.78E-09	2.94E-03	9.01E-06
PPVK05-05	1.00E-06	1.00E-09	1.00E-03	1.85E-06	7.69E-09	4.43E-04	6.31E-05
PPVK05-06	1.00E-06	1.00E-09	1.00E-03	3.05E-06	3.61E-09	2.57E-03	5.44E-06
PPVK05-07	1.00E-06	1.00E-09	1.00E-03	1.50E-06	1.51E-08	1.49E-04	9.19E-05

Apx Table A.3 Estimated porosity and relevant calibration statistics. "BACKPOR" represents the porosity assigned to all constant-head model cells (Figure 2.9). All calculations are based on the log-transformation of the parameters. The parameter names indicate the layer and the pilot point number in Figure 2.12, i.e., "PPVK02-01" is layer 2 (Upper Hutton), pilot point #1. Confidence limits are based on 95% confidence, i.e., +/- two standard deviations.

Name	Initial Value	Prior Confidence Limits		Estimated Value	Posterior Confidence Limits		Composite Scaled Sensitivity
		Lower	Upper		Lower	Upper	
BACKPOR	5.00E-02	2.89E-03	8.66E-01	4.70E-02	5.07E-03	4.37E-01	3.80E-05
PPOR02-01	5.00E-02	2.89E-03	8.66E-01	2.06E-02	9.49E-03	4.46E-02	2.86E-05
PPOR02-02	5.00E-02	2.89E-03	8.66E-01	1.83E-02	7.72E-03	4.32E-02	4.65E-05
PPOR02-03	5.00E-02	2.89E-03	8.66E-01	2.41E-02	1.94E-02	2.99E-02	4.41E-04
PPOR02-04	5.00E-02	2.89E-03	8.66E-01	4.95E-02	6.68E-03	3.67E-01	1.64E-05
PPOR02-05	5.00E-02	2.89E-03	8.66E-01	1.93E-02	1.73E-03	2.14E-01	3.42E-05
PPOR02-06	5.00E-02	2.89E-03	8.66E-01	1.08E-01	7.92E-02	1.46E-01	1.43E-04
PPOR02-07	5.00E-02	2.89E-03	8.66E-01	2.97E-02	3.15E-03	2.80E-01	9.51E-05
PPOR03-01	5.00E-02	2.89E-03	8.66E-01	1.62E-01	1.52E-01	1.72E-01	3.19E-04
PPOR03-02	5.00E-02	2.89E-03	8.66E-01	7.12E-02	6.32E-02	8.02E-02	1.92E-04
PPOR03-03	5.00E-02	2.89E-03	8.66E-01	3.00E-01	2.68E-01	3.35E-01	6.78E-05
PPOR03-04	5.00E-02	2.89E-03	8.66E-01	3.00E-01	1.85E-01	4.87E-01	2.07E-05
PPOR03-05	5.00E-02	2.89E-03	8.66E-01	5.91E-02	1.28E-02	2.73E-01	2.81E-05
PPOR03-06	5.00E-02	2.89E-03	8.66E-01	4.59E-03	5.51E-04	3.83E-02	3.20E-05
PPOR03-07	5.00E-02	2.89E-03	8.66E-01	3.43E-02	2.16E-02	5.43E-02	9.19E-04
PPOR04-01	5.00E-02	2.89E-03	8.66E-01	2.42E-02	1.92E-02	3.06E-02	1.49E-04
PPOR05-01	5.00E-02	2.89E-03	8.66E-01	5.37E-03	1.42E-03	2.03E-02	1.45E-04
PPOR05-02	5.00E-02	2.89E-03	8.66E-01	2.58E-03	1.57E-03	4.24E-03	3.27E-04
PPOR05-03	5.00E-02	2.89E-03	8.66E-01	1.80E-02	1.16E-02	2.81E-02	6.95E-04
PPOR05-04	5.00E-02	2.89E-03	8.66E-01	5.09E-02	4.51E-02	5.75E-02	1.71E-03
PPOR05-05	5.00E-02	2.89E-03	8.66E-01	7.64E-02	3.44E-02	1.70E-01	1.07E-04
PPOR05-06	5.00E-02	2.89E-03	8.66E-01	3.75E-02	3.42E-02	4.10E-02	1.03E-03
PPOR05-07	5.00E-02	2.89E-03	8.66E-01	3.54E-02	8.26E-03	1.52E-01	2.46E-04

CONTACT US

t 1300 363 400
+61 3 9545 2176
e enquiries@csiro.au
w www.csiro.au

YOUR CSIRO

Australia is founding its future on science and innovation. Its national science agency, CSIRO, is a powerhouse of ideas, technologies and skills for building prosperity, growth, health and sustainability. It serves governments, industries, business and communities across the nation.